International Journal of

Mathematics

and Physics

The International Journal of Mathematics and Physics is a peer-reviewed international journal covering all branches of mathematics and physics. The Journal welcomes papers on modern problems of mathematics and physics, in particular, Applied Mathematics, Algebra, Mathematical Analysis, Differential Equations, Mechanics, Informatics, Mathematical Modeling, Applied Physics, Radio Physics, Thermophysics, Nuclear Physics, Nanotechnology, and etc.

EDITORIAL

The most significant scientific achievements are attained through joint efforts of different sciences, mathematics and physics are among them. Therefore publication of the Journal, which shows results of current investigations in the field of mathematics and physics, will allow wider exhibition of scientific problems, tasks and discoveries.

One of the basic goals of the Journal is to promote extensive exchange of information between scientists from all over the world. We propose publishing service for original papers and materials of Mathematical and Physical Conferences (by selection) held in different countries and in the Republic of Kazakhstan.

Creation of the special International Journal of Mathematics and Physics is of great importance because a vast amount of scientists are willing to publish their articles and it will help to widen the geography of future dissemination. We will also be glad to publish papers of scientists from all the continents.

The Journal will publish experimental and theoretical investigations on Mathematics, Physical Technology and Physics. Among the subject emphasized are modern problems of Applied Mathematics, Algebra, Mathematical Analysis, Differential Equations, Mechanics, Informatics, Mathematical Modeling, Astronomy, Space Research, Theoretical Physics, Plasma Physics, Chemical Physics, Radio Physics, Thermophysics, Nuclear Physics, Nanotechnology, and etc.

The Journal is issued on the base of al-Farabi Kazakh National University. Leading scientists from different countries of the world agreed to join the Editorial Board of the Journal.

The Journal is published twice a year by al-Farabi Kazakh National University. We hope to receive papers from many laboratories which are interested in applications of the scientific principles of mathematics and physics and are carrying out researches on such subjects as production of new materials or technological problems.

S.N. Kharin[1,3*], T.A.Nauryz[1,2,3,4] iD, B. Miedzinski[5]

[1]Institute of Mathematics and Mathematical Modeling, Almaty, Kazakhstan
[2]Al-Farabi Kazakh National University, Almaty, Kazakhstan
[3]Kazakh-British Technical University, Almaty, Kazakhstam
[4]Satbayev University, Almaty, Kazakhstan
[5]Wroclaw University, Wroclaw, Poland
[*]e-mail: staskharin@yahoo.com

TWO PHASE SPHERICAL STEFAN INVERSE PROBLEM SOLUTION WITH LINEAR COMBINATION OF RADIAL HEAT POLYNOMIALS AND INTEGRAL ERROR FUNCTIONS IN ELECTRICAL CONTACT PROCESS

Abstract. In this research the inverse Stefan problem in spherical model where heat flux has to be determined is considered. This work is continuing of our research in electrical engineering that when heat flux passes through one material to the another material at the point where they contact heat distribution process takes the place. At free boundary $\alpha(t)$ contact spot starts to boiling and at $\beta(t)$ stars to melting and there appear two phase: liquid phase and solid phase. Our aim to calculate temperature in liquid and solid phase, then find heat flux entering into contact spot. The exact solution of problem represented in linear combination of series for radial heat polynomials and integral error functions. The recurrent formulas for determine unknown coefficients are represented. The effectiveness of method is checked by test problem and approximate problem in which exact solution and approximate solution of heat flux is compared. The coefficients of heat at liquid and solid phases and heat flux are found. The heat flux equation is checked by testing problem by using Mathcad program.
Key words: Stefan problem, radial heat polynomials, Faa-di Bruno, collocation method.

Introduction

Heat flux entering in electrical contact materials from electrical arc distributes radially and axially. Spherical model is most convenient, introduced by Holm R. [1], in the problem of heat distribution in electrical materials. In this problem generalized heat equation can be used. The generalized heat equation of the form

$$\frac{\partial \theta}{\partial t} = a_1^2 \frac{1}{r^v} \frac{\partial}{\partial x}\left(r^v \frac{\partial \theta}{\partial x}\right)$$

have the fundamental solution with delta-function containing initial condition by using Laplace transform can be represented as

$$G(x,y,t) = \frac{C_v}{2t}(xy)^{-\beta} e^{\frac{x^2+y^2}{4t}} I_\beta\left(\frac{xy}{2t}\right),$$

where

$$\beta = \frac{v-1}{2}, \quad C_v = 2^{-\beta}\Gamma(\beta+1)$$

We can consider the heat potentials related to this solution in form [2]

$$Q_{n,v}(x,t) = 2^{-\beta}\Gamma(\beta+1)^{-1}\int_0^\infty G(x,y,t)y^{2n+v}dy$$

and by using integration by parts method we have the following explicit formula of heat polynomials

$$Q_{n,v}(x,t) = \sum_{k=0}^n 2^{2k} \frac{n!\Gamma(\beta+1)x^{2(n-k)}t^k}{k!(n-k)!\Gamma(\beta+1+n-k)}$$

For applications it is convenient to multiply both sides of this equation by $\frac{\Gamma(\beta+1+n)}{\Gamma(\beta+1)}$ and we get the following solution

$$Q_{n,v}(x,t) = \sum_{k=0}^n 2^{2k} \frac{n!\Gamma(\beta+1+n)x^{2(n-k)}t^k}{k!(n-k)!\Gamma(\beta+1+n-k)}$$

which satisfy the generalized heat equation.

In this research we consider $v = 2$ which allow to transform to generalized heat equation to spherical heat equation [3]. The similar problems are considered in [4]-[7].

Mathematical model

Let us consider the liquid phase described in domain $\alpha(t) < r < \beta(t)$, $t > 0$ and solid phase in $\beta(t) < r < \infty$, $t > 0$ with spherical heat equations

$$\frac{\partial \theta_i}{\partial t} = a_i^2 \frac{1}{r^2} \frac{\partial}{\partial r}\left(r^2 \frac{\partial \theta_i}{\partial r}\right), \quad i = 1, 2 \qquad (1)$$

and each phase has initial condition as follows

$$\theta_1(\alpha(t), 0) = 0, \quad \alpha(0) = \beta(t) = 0, \qquad (2)$$

$$\theta_2(r, 0) = f(r), \quad f(0) = \theta_m. \qquad (3)$$

Heat flux entering $P(t)$ into spherical domain from electrical arc with radius r_0 in process pf heat transfer within electrical contact materials can be determined from condition

$$-\lambda_1 \frac{\partial \theta_1}{\partial r}\bigg|_{r=r_0} = P(t). \qquad (4)$$

Temperatures in liquid and solid phase at free boundary $\alpha(t)$ is equal to melting temperature

$$\theta_i(\beta(t), t) = \theta_m, \quad i = 1, 2. \qquad (5)$$

Motion of the free boundary can be calculated at Stefan's condition

$$-\lambda_1 \frac{\partial \theta_1}{\partial r}\bigg|_{r=\beta(t)} = -\lambda_2 \frac{\partial \theta_2}{\partial r}\bigg|_{r=\beta(t)} + L\gamma \frac{d\beta}{dt} \qquad (6)$$

and temperature of solid zone at infinity turns to zero

$$\theta_2\big|_{r=\infty} = 0. \qquad (7)$$

Problem solution

The solution of problem (1)-(7) we represent as linear combination of series for radial heat equation and integral error functions

$$\theta_1(r,t) = \sum_{n=0}^{\infty} A_n \sum_{k=0}^{n} \frac{2^{2k} n! \Gamma\left(\frac{3}{2}+n\right) r^{2(n-k)} t^k}{k!(n-k)! \Gamma\left(\frac{3}{2}+n-k\right)} +$$
$$+ \sum_{n=0}^{\infty} B_n \frac{(2a_1\sqrt{t})^{2n+1}}{r}\left(i^{2n+1}erfc\frac{-r}{2a_1\sqrt{t}} - i^{2n+1}erfc\frac{r}{2a_1\sqrt{t}}\right), \qquad (8)$$

$$\theta_1(r,t) = \sum_{n=0}^{\infty} C_n \sum_{k=0}^{n} \frac{2^{2k} n! \Gamma\left(\frac{3}{2}+n\right) r^{2(n-k)} t^k}{k!(n-k)! \Gamma\left(\frac{3}{2}+n-k\right)} +$$
$$+ \sum_{n=0}^{\infty} D_n \frac{(2a_2\sqrt{t})^{2n+1}}{r}\left(i^{2n+1}erfc\frac{-r}{2a_2\sqrt{t}} - i^{2n+1}erfc\frac{r}{2a_2\sqrt{t}}\right). \qquad (9)$$

The equations (8) and (9) satisfy heat equation (1) and undetermined coefficients A_n, B_n, C_n and D_n have to be founded to determine temperatures in phases. The function at initial condition for $\theta_2(r,t)$ is represented in expansion by Maclaurin series $f(r) = \sum_{n=0}^{\infty} \frac{f^{(n)}(0)}{n!} r^n$ and free boundaries can be considered in power series $\alpha(t) = \sum_{n=0}^{\infty} \alpha_n t^{n/2+1}$ and $\beta(t) = \sum_{n=0}^{\infty} \beta_n t^{n/2+1}$. Heat flux which have to be determined from condition (4) can be written in

$$P(t) = p_0 + p_1 t^{1/2} + p_2 t + p_3 t^{3/2} \ldots = \sum_{n=0}^{\infty} p_n t^{n/2}.$$

At first, we must find temperatures in liquid and solid zones, then by using property of integral error function to condition (3) we get

$$\sum_{n=0}^{\infty} C_n r^{2n} + \sum_{n=0}^{\infty} D_n \frac{2}{(2n+1)!} r^{2n} = \sum_{n=0}^{\infty} \frac{f^{(n)}(0)}{n!} r^n \quad (10)$$

By comparing the power of r in both sides (10) we obtain the following form

$$C_n + D_n \frac{2}{(2n+1)!} = \frac{f^{(2n)}(0)}{(2n)!} \qquad (11)$$

and from conditions (5) we have

$$\sum_{n=0}^{\infty} A_n \sum_{k=0}^{n} \frac{2^{2k} n! \Gamma\left(\frac{3}{2}+n\right) \beta(\tau)^{2(n-k)} \tau^{2k}}{k!(n-k)! \Gamma\left(\frac{3}{2}+n-k\right)} + \qquad (12)$$

$$+ \sum_{n=0}^{\infty} B_n \frac{(2a_1\tau)^{2n+1}}{\beta(\tau)} \left(i^{2n+1} erfc(-\upsilon(\tau)) - i^{2n+1} erfc(\upsilon(\tau))\right) = \theta_m,$$

$$\sum_{n=0}^{\infty} C_n \sum_{k=0}^{n} \frac{2^{2k} n! \Gamma\left(\frac{3}{2}+n\right) \beta(\tau)^{2(n-k)} \tau^{2k}}{k!(n-k)! \Gamma\left(\frac{3}{2}+n-k\right)} + \qquad (13)$$

$$+ \sum_{n=0}^{\infty} D_n \frac{(2a_2\tau)^{2n+1}}{\beta(\tau)} \left(i^{2n+1} erfc(-\upsilon(\tau)) - i^{2n+1} erfc(\upsilon(\tau))\right) = \theta_m,$$

and from Stefan's condition we obtain

$$-\lambda_1 \left[\sum_{n=0}^{\infty} A_n \sum_{k=0}^{n} \frac{2^{2k} n! \Gamma\left(\frac{3}{2}+n\right) 2(n-k)\beta(\tau)^{2(n-k)-1} \tau^{2k}}{k!(n-k)! \Gamma\left(\frac{3}{2}+n-k\right)} + \sum_{n=0}^{\infty} B_n \left(-\frac{(2a_1\tau)^{2n+1}}{\beta^2(\tau)} \left(i^{2n+1} erfc(-\upsilon(\tau)) - i^{2n+1} erfc(\upsilon(\tau))\right) \right. \right.$$

$$\left. \left. - \frac{(2a_1\tau)^{2n}}{\alpha(\tau)} \left(i^{2n} erfc(-\upsilon(\tau)) + i^{2n} erfc(\upsilon(\tau))\right) \right) \right] = -\lambda_2 \left[\sum_{n=0}^{\infty} C_n \sum_{k=0}^{n} \frac{2^{2k} n! \Gamma\left(\frac{3}{2}+n\right) 2(n-k)\beta(\tau)^{2(n-k)-1} \tau^{2k}}{k!(n-k)! \Gamma\left(\frac{3}{2}+n-k\right)} + \right. \qquad (14)$$

$$\left. + \sum_{n=0}^{\infty} D_n \left(-\frac{(2a_2\tau)^{2n+1}}{\beta^2(\tau)} \left(i^{2n+1} erfc(-\upsilon(\tau)) - i^{2n+1} erfc(\upsilon(\tau))\right) - \frac{(2a_2\tau)^{2n}}{\beta(\tau)} \left(i^{2n} erfc(-\upsilon(\tau)) + i^{2n} erfc(\upsilon(\tau))\right) \right) \right] + L\gamma \frac{d\beta}{d\tau},$$

where $\sqrt{t} = \tau$ and

$$\upsilon(\tau) = \frac{\beta_0 + \beta_1 \tau + \beta_2 \tau^2 + ...}{2a_1} = \frac{1}{2a_1} \sum_{n=0}^{\infty} \upsilon_n \tau^n.$$

Firstly, we take l-th derivative both sides of (13) when $\tau = 0$ using Leibniz rule for first and second term of (13)

$$\left. \frac{\partial^l \left[\tau^{2k} \beta(\tau)^{2(n-k)} \right]}{\partial \tau^l} \right|_{\tau=0} = \frac{l!}{(l-2k)!} [\beta(\tau)]^{(2n-4k-l)}, \quad (15)$$

$$\left. \frac{\partial^l \left[\tau^{2k+1} \left[i^{2n+1} erfc(-\upsilon(\tau)) - i^{2n+1} erfc(\upsilon(\tau)) \right] \right]}{\partial \tau^l} \right|_{\tau=0} = $$

$$= \frac{l!}{(l-2k-1)!} \left[i^{2n+1} erfc(-\upsilon(\tau)) - i^{2n+1} erfc(\upsilon(\tau)) \right]^{l-2k-1}. \qquad (16)$$

Using Faa-di Bruno for (15) and (16) we get

$$\left. \frac{l!}{(l-2k)!} [\beta(\tau)]^{(l-2n)} \right|_{\tau=0} =$$

$$= \frac{l!}{(l-2k)!} \sum_{m=1}^{l-2n} \beta_0^{(m)} \sum_{b_i} \frac{(l-2k-1)! \beta_1^{b_1} \beta_2^{b_2} ... \beta_{l-2n+1}^{b_{l-2n+1}}}{b_1! b_2! ... b_{l-2n+1}!}, \qquad (17)$$

$$\left. \frac{l!}{(l-2k-1)!} \left[i^{2n+1} erfc(-\upsilon(\tau)) - i^{2n+1} erfc(\upsilon(\tau)) \right]^{l-2k-1} \right|_{\tau=0} =$$

$$= \frac{l!}{(l-2k-1)!} \sum_{m=1}^{l-2k-1} \left[i^{2n+1} erfc(-\upsilon_0) - i^{2n+1} erfc(\upsilon_0) \right]^{(m)} \times \qquad (18)$$

$$\times \sum_{b_i} \frac{(l-2k-1)! \upsilon_1^{b_1} \upsilon_2^{b_2} ... \upsilon_{l-2n}^{b_{l-2n}}}{b_1! b_2! ... b_{l-2k}!}.$$

From system of equations (11) and (13) we determine the coefficients C_n, D_n. Multiplying both sides of (13) by $\beta(\tau)$ we have

$$\sum_{n=0}^{\infty} C_n \sum_{k=0}^{n} \frac{2^{2k} n! \Gamma\left(\frac{3}{2}+n\right) \beta(\tau)^{2(n-k)+1} \tau^{2k}}{k!(n-k)! \Gamma\left(\frac{3}{2}+n-k\right)} +$$

$$+ \sum_{n=0}^{\infty} D_n (2a_2\tau)^{2n+1} \left(i^{2n+1} erfc(-\upsilon(\tau)) - i^{2n+1} erfc(\upsilon(\tau))\right) =$$

$$= \theta_m \beta(\tau),$$

Taking l-th derivative both sides of this expression and using (10) we have

$$D_n = \frac{(2n+1)! \left[\theta_m \beta_l l! (2n)! - f^{(2n)}(0) \delta_{n,l} \right]}{2(2n)! \xi_{n,l}}, \quad (19)$$

$$C_n = \frac{f^{(2n)}(0)}{(2n)!} - \frac{2}{(2n+1)!}\frac{(2n+1)!\left[\theta_m\beta_l l!(2n)! - f^{(2n)}(0)\delta_{n,l}\right]}{2(2n)!\xi_{n,l}}, \quad (20)$$

where

$$\delta_{n,l} = \frac{2^{2k}n!\Gamma\left(\frac{3}{2}+n\right)}{k!(n-k)!\Gamma\left(\frac{3}{2}+n-k\right)}\frac{l!}{(l-2k)!}\times$$

$$\times\sum_{m=1}^{l-2n}\beta_0^{(m)}\sum_{b_i}\frac{(l-2k-1)!\beta_1^{b_1}\beta_2^{b_2}...\beta_{l-2n+1}^{b_{l-2n+1}}}{b_1!b_2!...b_{l-2n+1}!},$$

$$\xi_{n,l} = \frac{(2a_1)^{2n+1}l!}{(l-2k-1)!}\sum_{m=1}^{l-2k-1}\left[i^{2n+1}erfc(-\upsilon_0) - i^{2n+1}erfc(\upsilon_0)\right]^{(m)}\times$$

$$\times\sum_{b_i}\frac{(l-2k-1)!\upsilon_1^{b_1}\upsilon_2^{b_2}...\upsilon_{l-2n}^{b_{l-2n}}}{b_1!b_2!...b_{l-2k}!}.$$

Multiplying $\beta(\tau)$ both sides of (12) and (14) we have

$$\sum_{n=0}^{\infty}A_n\sum_{k=0}^{n}\frac{2^{2k}n!\Gamma\left(\frac{3}{2}+n\right)\beta(\tau)^{2(n-k)+1}\tau^{2k}}{k!(n-k)!\Gamma\left(\frac{3}{2}+n-k\right)}+$$

$$+\sum_{n=0}^{\infty}B_n(2a_1\tau)^{2n+1}\left(i^{2n+1}erfc(-\upsilon(\tau)) - i^{2n+1}erfc(\upsilon(\tau))\right) = \quad (21)$$

$$= \theta_m\beta(\tau),$$

$$-\lambda_1\left[\sum_{n=0}^{\infty}A_n\sum_{k=0}^{n}\frac{2^{2k}n!\Gamma\left(\frac{3}{2}+n\right)2(n-k)\beta(\tau)^{2(n-k)}\tau^{2k}}{k!(n-k)!\Gamma\left(\frac{3}{2}+n-k\right)} - \sum_{n=0}^{\infty}B_n(2a_1\tau)^{2n}\left(i^{2n}erfc(-\upsilon(\tau)) + i^{2n}erfc\upsilon(\tau)\right)\right] =$$

$$= -\lambda_2\left[\sum_{n=0}^{\infty}C_n\sum_{k=0}^{n}\frac{2^{2k}n!\Gamma\left(\frac{3}{2}+n\right)2(n-k)\beta(\tau)^{2(n-k)}\tau^{2k}}{k!(n-k)!\Gamma\left(\frac{3}{2}+n-k\right)} - \sum_{n=0}^{\infty}D_n(2a_2\tau)^{2n}\left(i^{2n}erfc(-\upsilon(\tau)) + i^{2n}erfc(\upsilon(\tau))\right)\right] \quad (22)$$

$$+(\lambda_2-\lambda_1)\theta_m+\frac{L\gamma}{2}\nu(\beta)_m,$$

where $\beta'(\tau)\beta(\tau) = \frac{1}{2}\frac{d}{dr}\beta^2(\tau)$ and

$$\beta^2(\tau) = \sum_{n=0}^{\infty}\nu(\beta)_m\tau^n, \quad \nu(\beta)_0 = \beta_0^2,$$

$$\nu(\beta)_m = \frac{1}{m\beta_0}\sum_{k=1}^{m}(3k-m)\beta_k\nu(\beta)_{m-k}, \quad m \geq 1$$

Taking l-th derivative both sides of equations (21) and (22) at $\tau = 0$ we get

$$\sum_{n=0}^{l}A_n\sum_{k=0}^{n}\frac{2^{2k}n!\Gamma\left(\frac{3}{2}+n\right)}{k!(n-k)!\Gamma\left(\frac{3}{2}+n-k\right)}\frac{l!}{(l-2k)!}\sum_{m=1}^{l-2n}\beta_0^{(m)}\sum_{b_i}\frac{(l-2k-1)!\beta_1^{b_1}\beta_2^{b_2}...\beta_{l-2n+1}^{b_{l-2n+1}}}{b_1!b_2!...b_{l-2n+1}!}$$

$$+\sum_{n=0}^{l}B_n\frac{(2a_1)^{2n+1}l!}{(l-2k-1)!}\sum_{m=1}^{l-2k-1}\left[i^{2n+1}erfc(-\upsilon_0)-i^{2n+1}erfc(\upsilon_0)\right]^{(m)}\sum_{b_i}\frac{(l-2k-1)!\upsilon_1^{b_1}\upsilon_2^{b_2}...\upsilon_{l-2n}^{b_{l-2n}}}{b_1!b_2!...b_{l-2k}!} = \theta_m\beta_l l! \quad (23)$$

and

$$-\lambda_1\left[2\sum_{n=0}^{l}A_n\sum_{k=0}^{n}\frac{2^{2k}n!\Gamma\left(\frac{3}{2}+n\right)2(n-k)}{k!(n-k)!\Gamma\left(\frac{3}{2}+n-k\right)}\frac{l!}{(l-2k)!}\sum_{m=1}^{l-2n}\beta_0^{(m)}\sum_{b_i}\frac{(l-2k)!\beta_1^{b_1}\beta_2^{b_2}...\beta_{l-2n+1}^{b_{l-2n+1}}}{b_1!b_2!...b_{l-2n+1}!}-\right.$$

$$\left.-\sum_{n=0}^{l}B_n\frac{(2a_1)^{2n+1}l!}{(l-2n)!}\sum_{m=1}^{l-2n}\left[(-1)^m i^{2n-m}erfc(-\upsilon_0)-i^{2n}erfc(\upsilon_0)\right]^{(m)}\sum_{b_i}\frac{(l-2n)!\upsilon_1^{b_1}\upsilon_2^{b_2}...\upsilon_{l-2n+1}^{b_{l-2n+1}}}{b_1!b_2!...b_{l-2n+1}!}\right]=$$

$$=-\lambda_2\left[2\sum_{n=0}^{l}C_n\sum_{k=0}^{n}\frac{2^{2k}n!\Gamma\left(\frac{3}{2}+n\right)2(n-k)}{k!(n-k)!\Gamma\left(\frac{3}{2}+n-k\right)}\frac{l!}{(l-2k)!}\sum_{m=1}^{l-2n}\beta_0^{(m)}\sum_{b_i}\frac{(l-2k)!\beta_1^{b_1}\beta_2^{b_2}...\beta_{l-2n+1}^{b_{l-2n+1}}}{b_1!b_2!...b_{l-2n+1}!}-\right.$$

$$\left.-\sum_{n=0}^{l}D_n\frac{(2a_2)^{2n+1}l!}{(l-2n)!}\sum_{m=1}^{l-2n}\left[(-1)^m i^{2n-m}erfc(-\upsilon_0)-i^{2n}erfc(\upsilon_0)\right]^{(m)}\sum_{b_i}\frac{(l-2n)!\upsilon_1^{b_1}\upsilon_2^{b_2}...\upsilon_{l-2n+1}^{b_{l-2n+1}}}{b_1!b_2!...b_{l-2n+1}!}+\frac{L\gamma}{2}l!\nu(\beta)_{l+1}\right]$$

(24)

From recurrent equations (23) and (24) we can determined the coefficients A_n and B_n as free boundary is known.

$$A_n=\frac{\theta_m\beta_l l!-B_n\eta_{n,l}}{\omega_{n,l}},\quad B_n=\frac{\chi_{n,l}+2\lambda_1\dfrac{\theta_m\beta_l l!\vartheta_{n,l}}{\omega_{n,l}}}{\lambda_1\left[2\dfrac{\eta_{n,l}}{\omega_{n,l}}\vartheta_{n,l}+\zeta_{n,l}\right]}$$

(25)

where

$$\eta_{n,l}=\frac{(2a_1)^{2n+1}l!}{(l-2k-1)!}\sum_{m=1}^{l-2k-1}\left[i^{2n+1}erfc(-\upsilon_0)-i^{2n+1}erfc(\upsilon_0)\right]^{(m)}\times\sum_{b_i}\frac{(l-2k-1)!\upsilon_1^{b_1}\upsilon_2^{b_2}...\upsilon_{l-2n}^{b_{l-2n}}}{b_1!b_2!...b_{l-2k}!},$$

$$\omega_{n,l}=\sum_{k=0}^{n}\frac{2^{2k}n!\Gamma\left(\frac{3}{2}+n\right)}{k!(n-k)!\Gamma\left(\frac{3}{2}+n-k\right)}\frac{l!}{(l-2k)!}\times\sum_{m=1}^{l-2n}\beta_0^{(m)}\sum_{b_i}\frac{(l-2k-1)!\beta_1^{b_1}\beta_2^{b_2}...\beta_{l-2n+1}^{b_{l-2n+1}}}{b_1!b_2!...b_{l-2n+1}!},$$

$$\chi_{n,l}=-\lambda_2\left[2\sum_{n=0}^{l}C_n\sum_{k=0}^{n}\frac{2^{2k}n!\Gamma\left(\frac{3}{2}+n\right)2(n-k)}{k!(n-k)!\Gamma\left(\frac{3}{2}+n-k\right)}\frac{l!}{(l-2k)!}\sum_{m=1}^{l-2n}\beta_0^{(m)}\sum_{b_i}\frac{(l-2k)!\beta_1^{b_1}\beta_2^{b_2}...\beta_{l-2n+1}^{b_{l-2n+1}}}{b_1!b_2!...b_{l-2n+1}!}-\right.$$

$$\left.-\sum_{n=0}^{l}D_n\frac{(2a_2)^{2n+1}l!}{(l-2n)!}\sum_{m=1}^{l-2n}\left[(-1)^m i^{2n-m}erfc(-\upsilon_0)-i^{2n}erfc(\upsilon_0)\right]^{(m)}\sum_{b_i}\frac{(l-2n)!\upsilon_1^{b_1}\upsilon_2^{b_2}...\upsilon_{l-2n+1}^{b_{l-2n+1}}}{b_1!b_2!...b_{l-2n+1}!}\right]+\frac{L\gamma}{2}l!\nu(\beta)_{l+1},$$

$$\zeta_{n,l}=\frac{(2a_1)^{2n+1}l!}{(l-2n)!}\sum_{m=1}^{l-2n}\left[(-1)^m i^{2n-m}erfc(-\upsilon_0)-i^{2n}erfc(\upsilon_0)\right]^{(m)}\times\sum_{b_i}\frac{(l-2n)!\upsilon_1^{b_1}\upsilon_2^{b_2}...\upsilon_{l-2n+1}^{b_{l-2n+1}}}{b_1!b_2!...b_{l-2n+1}!}.$$

From condition at heat flux entering we have the following equation

$$-\lambda_1 \left[\sum_{n=0}^{\infty} B_n \left(-\frac{(2a_1\tau)^{2n+1}}{\alpha^2(\tau)} \left(i^{2n+1}erfc(-\varphi(\tau)) - i^{2n+1}erfc(\varphi(\tau)) \right) - \frac{(2a_1\tau)^{2n}}{\alpha(\tau)} \left(i^{2n}erfc(-\varphi(\tau)) + i^{2n}erfc(\varphi(\tau)) \right) \right) + \right.$$
$$\left. + \sum_{n=0}^{l} A_n \sum_{k=0}^{n} \frac{2^{2k} n! \Gamma\left(\frac{3}{2}+n\right) 2(n-k)}{k!(n-k)! \Gamma\left(\frac{3}{2}+n-k\right)} \alpha(\tau)^{2(n-k)-1} \tau^{2n-1} \right] = \sum_{n=0}^{\infty} p_n \tau^n \qquad (26)$$

Multiplying both sides by $\alpha^2(\tau)$ we obtain the next equation

$$-\lambda_1 \left[\sum_{n=0}^{\infty} B_n \left(-(2a_1\tau)^{2n+1} \left(i^{2n+1}erfc(-\varphi(\tau)) - i^{2n+1}erfc(\varphi(\tau)) \right) - (2a_1\tau)^{2n} \alpha(\tau) \left(i^{2n}erfc(-\varphi(\tau)) + i^{2n}erfc(\varphi(\tau)) \right) \right) + \right.$$
$$\left. + \sum_{n=0}^{l} A_n \sum_{k=0}^{n} \frac{2^{2k} n! \Gamma\left(\frac{3}{2}+n\right) 2(n-k)}{k!(n-k)! \Gamma\left(\frac{3}{2}+n-k\right)} \alpha(\tau)^{2(n-k)+1} \tau^{2n-1} \right] = \sum_{n=0}^{\infty} p_n \tau^n u^2(\tau) \qquad (27)$$

where $\varphi(\tau) = \dfrac{\alpha_0 + \alpha_1 \tau + \alpha_2 \tau^2 + ...}{2a_1} = \dfrac{1}{2a_1} \sum_{n=0}^{\infty} \varphi_n \tau^n$ and

$$\alpha^2(\tau) = \sum_{n=0}^{\infty} u(\alpha)_m \tau^n, \quad u(\alpha)_0 = \alpha_0^2, \quad u(\alpha)_m = \frac{1}{m\alpha_0} \sum_{k=1}^{m} (3k-m)\alpha_k u(\alpha)_{m-k}, \quad m \ge 1.$$

Analogously, taking l-th derivative of both sides of equation (27) we have

$$-\lambda_1 \left[\sum_{n=0}^{l} B_n \left\{ -\frac{(2a_1)^{2n+1} l!}{(l-2n-1)!} \sum_{m=1}^{l-2n-1} \left((-1)^m i^{2n+1-m}erfc(-\varphi_0) - i^{2n+1-m}erfc(\varphi_0) \right) \sum_{b_i} \frac{(l-2n)! \varphi_1^{b_1} \varphi_2^{b_2} ... \varphi_{l-2n+1}^{b_{l-2n+1}}}{b_1! b_2! ... b_{l-2n+1}!} - \right. \right.$$

$$-\frac{(2a_1)^{2n} l!}{(l-2n)!} \sum_{m=1}^{l-2n} \binom{l-2n}{m} [\alpha_0]^{(m)} \sum_{b_i} \frac{(l-2n)! \alpha_1^{b_1} \alpha_2^{b_2} ... \alpha_{l-2n+1}^{b_{l-2n+1}}}{b_1! b_2! ... b_{l-2n+1}!} \sum_{p=1}^{l-2n-m} (-1)^p \left(i^{2n-p}erfc(-\varphi_0) + \right.$$

$$\left. + i^{2n-p}erfc(-\varphi_0) \right) \sum_{b_i} \frac{(l-2n)! \varphi_1^{b_1} \varphi_2^{b_2} ... \varphi_{l-2n+1}^{b_{l-2n+1}}}{b_1! b_2! ... b_{l-2n+1}!} \right\} - \sum_{n=0}^{l} A_n \sum_{k=0}^{n} \frac{2^{2k} n! \Gamma\left(\frac{3}{2}+n\right) 2(n-k)}{k!(n-k)! \Gamma\left(\frac{3}{2}+n-k\right)} \frac{l!}{(l-2n+1)!} \qquad (28)$$

$$\left. \cdot (2n-2k+1)! \sum_{m=1}^{l-2n+1} \alpha_0^{4n-2k-l} \sum_{b_i} \frac{(l-2n+1)! \varphi_1^{b_1} \varphi_2^{b_2} ... \varphi_{l-2n+2}^{b_{l-2n+2}}}{b_1! b_2! ... b_{l-2n+2}!} \right] = \sum_{n=0}^{l} p_n \frac{l!}{2(l-n)!} l! u(\alpha_0)_{l+1}$$

From recurrent equation (28) we can determine the coefficients of heat flux in process of electrical contact materials.

Exact solution of test problem

In this section we consider test problem to check effectiveness of method of radial heat polynomials and integral error functions for inverse problem of spherical Stefan problem (1)-(7). The free boundaries are given in the form $\alpha(t) = \alpha_0 \sqrt{t}$ and $\beta(t) = \beta_0 \sqrt{t}$, then from the initial condition (3) and boundary condition (6) we have

$$C_n + D_n \frac{2}{(2n+1)!} = \frac{f^{(2n)}(0)}{(2n)!} \tag{29}$$

$$\sum_{n=0}^{\infty} C_n \sum_{k=0}^{n} \frac{2^{2k} n! \Gamma\left(\frac{3}{2}+n\right) \beta_0^{2(n-k)} t^n}{k!(n-k)! \Gamma\left(\frac{3}{2}+n-k\right)} + $$
$$+ \sum_{n=0}^{\infty} D_n \frac{(2a_1)^{2n+1}}{\beta_9} \left(i^{2n+1} erfc \frac{-\beta_0}{2a_1} - i^{2n+1} erfc \frac{\beta_0}{2a_1} \right) = \theta_m, \tag{30}$$

$$\sum_{n=0}^{\infty} A_n \sum_{k=0}^{n} \frac{2^{2k} n! \Gamma\left(\frac{3}{2}+n\right) \beta_0^{2(n-k)} t^n}{k!(n-k)! \Gamma\left(\frac{3}{2}+n-k\right)} + $$
$$+ \sum_{n=0}^{\infty} B_n \frac{(2a_2)^{2n+1}}{\beta_9} \left(i^{2n+1} erfc \frac{-\beta_0}{2a_2} - i^{2n+1} erfc \frac{\beta_0}{2a_2} \right) = \theta_m, \tag{31}$$

and from Stefan's condition at free boundary $\beta(t)$ we obtain

$$-\lambda_1 \left[2 \sum_{n=0}^{\infty} A_n \sum_{k=0}^{n} \frac{2^{2k} n! \Gamma\left(\frac{3}{2}+n\right) 2(n-k) \beta_0^{2(n-k)}}{k!(n-k)! \Gamma\left(\frac{3}{2}+n-k\right)} t^n - \sum_{n=0}^{\infty} B_n (2a_1\sqrt{t})^n \left(i^{2n} erfc \frac{-\beta_0}{2a_1} + i^{2n} erfc \frac{\beta_0}{2a_1} \right) \right] = $$

$$= -\lambda_1 \left[2 \sum_{n=0}^{\infty} C_n \sum_{k=0}^{n} \frac{2^{2k} n! \Gamma\left(\frac{3}{2}+n\right) 2(n-k) \beta_0^{2(n-k)}}{k!(n-k)! \Gamma\left(\frac{3}{2}+n-k\right)} t^n - \sum_{n=0}^{\infty} D_n (2a_2\sqrt{t})^n \left(i^{2n} erfc \frac{-\beta_0}{2a_2} + i^{2n} erfc \frac{\beta_0}{2a_2} \right) \right] + \tag{32}$$

$$+ (\lambda_2 - \lambda_1)\theta_m + \frac{L\gamma}{2} \beta_0^2$$

For $n = 0$ from system of equations (28)-(29) we have

$$C_0 = f(0) - \frac{\theta_m - f(0)}{\frac{a_2}{\beta_0}\left(i^1 erfc \frac{-\beta_0}{2a_2} - i^1 erfc \frac{\beta_0}{2a_2} \right) - 1} \tag{33}$$

$$D_0 = \frac{\theta_m - f(0)}{\frac{2a_2}{\beta_0}\left(i^1 erfc \frac{-\beta_0}{2a_2} - i^1 erfc \frac{\beta_0}{2a_2} \right) - 2} \tag{34}$$

and from system of equations (30)-(31) we obtain

$$B_0 = \frac{\lambda_1 D_0 \left(i^0 erfc \frac{-\beta_0}{2a_2} + i^0 erfc \frac{\beta_0}{2a_2} \right) + (\lambda_2 - \lambda_1)\theta_m + \frac{L\gamma}{2}\beta_0^2}{\lambda_1 \left(i^0 erfc \frac{-\beta_0}{2a_1} + i^0 erfc \frac{\beta_0}{2a_1} \right)} \tag{35}$$

$$A_0 = \theta_m - B_0 \frac{2a_1}{\beta_0}\left(i^0 erfc \frac{-\beta_0}{2a_2} + i^0 erfc \frac{\beta_0}{2a_2} \right). \tag{36}$$

For $n \geq 1$ we have the following results

$$D_n = \frac{-\dfrac{f^{(2n)}(0)}{(2n)!}\displaystyle\sum_{k=0}^{n}\dfrac{2^{2k}n!\Gamma\left(\dfrac{3}{2}+n\right)\beta_0^{2(n-k)}}{k!(n-k)!\Gamma\left(\dfrac{3}{2}+n-k\right)}}{\dfrac{(2a_2)^{2n+1}}{\beta_0}\left(i^{2n+1}erfc\dfrac{-\beta_0}{2a_2}-i^{2n+1}erfc\dfrac{\beta_0}{2a_2}\right)-\dfrac{2}{(2n+1)!}\displaystyle\sum_{k=0}^{n}\dfrac{2^{2k}n!\Gamma\left(\dfrac{3}{2}+n\right)\beta_0^{2(n-k)}}{k!(n-k)!\Gamma\left(\dfrac{3}{2}+n-k\right)}} \tag{37}$$

Using this result and put in (29) we can find coefficient C_n directly. And for other coefficients we get

$$B_n = \frac{\lambda_2\left[D_n(2a_2)^{2n}\left(i^{2n}erfc\dfrac{-\beta_0}{2a_2}+i^{2n}erfc\dfrac{-\beta_0}{2a_2}\right)-C_n\displaystyle\sum_{k=0}^{n}\dfrac{2^{2k}n!\Gamma\left(\dfrac{3}{2}+n\right)2(n-k)\beta_0^{2(n-k)}}{k!(n-k)!\Gamma\left(\dfrac{3}{2}+n-k\right)}\right]}{\lambda_1\left[\dfrac{\dfrac{2(2a_1)^{2n+1}}{\beta_0}\left(i^{2n+1}erfc\dfrac{-\beta_0}{2a_1}-i^{2n}erfc\dfrac{\beta_0}{2a_1}\right)}{\displaystyle\sum_{k=0}^{n}\dfrac{2^{2k}n!\Gamma\left(\dfrac{3}{2}+n\right)\beta_0^{2(n-k)}}{k!(n-k)!\Gamma\left(\dfrac{3}{2}+n-k\right)}}\displaystyle\sum_{k=0}^{n}\dfrac{2^{2k}n!\Gamma\left(\dfrac{3}{2}+n\right)2(n-k)\beta_0^{2(n-k)}}{k!(n-k)!\Gamma\left(\dfrac{3}{2}+n-k\right)}-(2a_1)^{2n}\left(i^{2n}erfc\dfrac{-\beta_0}{2a_1}+i^{2n}erfc\dfrac{-\beta_0}{2a_1}\right)\right]} \tag{38}$$

and

$$A_n = -B_n\frac{\dfrac{(2a_1)^{2n+1}}{\beta_0}\left(i^{2n+1}erfc\dfrac{-\beta_0}{2a_1}-i^{2n+1}erfc\dfrac{-\beta_0}{2a_1}\right)}{\displaystyle\sum_{k=0}^{n}\dfrac{2^{2k}n!\Gamma\left(\dfrac{3}{2}+n\right)\beta_0^{2(n-k)}}{k!(n-k)!\Gamma\left(\dfrac{3}{2}+n-k\right)}} \tag{39}$$

Heat flux can be determined form condition (3) which takes the form

$$-\lambda_1\left[\sum_{n=0}^{\infty}A_n\sum_{k=0}^{n}\frac{2^{2k}n!\Gamma\left(\dfrac{3}{2}+n\right)2(n-k)\alpha_0^{2(n-k)-1}t^{n-\frac{1}{2}}}{k!(n-k)!\Gamma\left(\dfrac{3}{2}+n-k\right)}-\sum_{n=0}^{\infty}B_n\left(\frac{(2a_1)^{2n+1}t^{n-\frac{1}{2}}}{\alpha_0^2}\left(i^{2n+1}erfc\frac{-\alpha_0}{2a_1}-i^{2n+1}erfc\frac{\alpha_0}{2a_1}\right)-\right.\right.$$
$$\left.\left.+\frac{(2a_1)^{2n}t^{n-\frac{1}{2}}}{\alpha_{00}}\left(i^{2n}erfc\frac{-\alpha_0}{2a_1}+i^{2n}erfc\frac{\alpha_0}{2a_1}\right)\right)\right]=\sum_{n=0}^{\infty}p_n t^{\frac{n}{2}} \tag{40}$$

Then from expression (40) we obtain the coefficients of heat flux passes through liquid and solid phases

$$\begin{cases} p_1 = -\lambda_1 \left[A_1 2\alpha_0 - B_1 \left(\frac{(2a_1)^3}{\alpha_0^2} \left(i^3 erfc \frac{-\alpha_0}{2a_1} - i^3 erfc \frac{\alpha_0}{2a_1} \right) + \frac{(2a_1)^2}{\alpha_0} \left(i^2 erfc \frac{-\alpha_0}{2a_1} + i^2 erfc \frac{\alpha_0}{2a_1} \right) \right) \right] \\[2ex] p_3 = -\lambda_1 \left[A_2 (4\alpha_0^3 + 40\alpha_0) - B_2 \left(\frac{(2a_1)^5}{\alpha_0^2} \left(i^5 erfc \frac{-\alpha_0}{2a_1} - i^5 erfc \frac{\alpha_0}{2a_1} \right) + \frac{(2a_1)^4}{\alpha_0} \left(i^4 erfc \frac{-\alpha_0}{2a_1} + i^4 erfc \frac{\alpha_0}{2a_1} \right) \right) \right] \\[2ex] p_5 = -\lambda_1 \left[A_3 (6\alpha_0^5 + 168\alpha_0^3 + 840\alpha_0) - B_3 \left(\frac{(2a_1)^7}{\alpha_0^2} \left(i^7 erfc \frac{-\alpha_0}{2a_1} - i^7 erfc \frac{\alpha_0}{2a_1} \right) + \frac{(2a_1)^6}{\alpha_0} \left(i^6 erfc \frac{-\alpha_0}{2a_1} + i^6 erfc \frac{\alpha_0}{2a_1} \right) \right) \right] \\[2ex] \vdots \\ \dotfill \\[2ex] p_{2n+1} = -\lambda_1 \left[A_{n+1} \sum_{k=0}^{n+1} \frac{2^{2k}(n+1)!\,\Gamma\!\left(\frac{5}{2}+n\right) 2(n-k+1)\alpha_0^{2(n-k)+1}}{k!(n-k+1)!\,\Gamma\!\left(\frac{5}{2}+n-k\right)} - B_{n+1} \left(\frac{(2a_1)^{2n+3}}{\alpha_0^2} \left(i^{2n+3} erfc \frac{-\alpha_0}{2a_1} - i^{2n+3} erfc \frac{\alpha_0}{2a_1} \right) + \right. \right. \\[3ex] \left. \left. \hspace{4cm} + \frac{(2a_1)^{2n+2}}{\alpha_0} \left(i^{2n+2} erfc \frac{-\alpha_0}{2a_1} + i^{2n+2} erfc \frac{\alpha_0}{2a_1} \right) \right) \right] \end{cases} \tag{41}$$

and even indexed coefficients of heat flux $p_{2n} = 0$. By using Mathcad 15 and taking $a_1 = a_2 = L = \gamma = \alpha_0 = \beta_0 = \lambda_1 = \lambda_2 = 1$ and melting temperature θ_m we get exact values of first three coefficients of temperature in two phase $A_1 = B_1 = C_1 = D_1 = C_0 = D_0 = 0$ and $A_2 = C_2 = -1.574 \times 10^{-4}$, $B_2 = D_2 = 9.442 \times 10^{-3}$ are calculated from system of equations (33)-(39). Then first three coefficients of heat flux is $p_0 = p_1 = 0$ and $p_2 = 0.057$ which can be found from (41).

Approximate solution of test problem

In this section we consider collocation method that useful to engineers for testing and we try to show that by using three points $t = 0$, $t = 0.5$ and $t = 1$ we can obtain no

error estimates. Let $a_1 = a_2 = L = \gamma = 1$ and $\theta_m = 0$, then for calculation Mathcad 15 is used and we get the next approximate coefficients for temperature in liquid and solid zones $A_0 = -0.25$, $B_0 = 0.125$, $A_1 = B_1 = C_1 = D_1 = C_0 = D_0 = 0$ and $A_2 = C_2 = -1.574 \times 10^{-4}$, $B_2 = D_2 = 9.442 \times 10^{-3}$. Then approximate values of first three heat flux is similar to exact values. The Fig.1 shows the graphs of approximate heat flux (approx_P(t)) and exact heat flux (exact_P(t)).

By calculating relative error with Mathcad 15 we get Fig.2 in which we can see that that at each point $t = 0$, $t = 0.5$, $t = 1$ we have zero error estimate function (Err(t))

Then we can summarize that method radial heat polynomials and integral error functions is the most effective in the heat transfer problem appearing in electrical contact process.
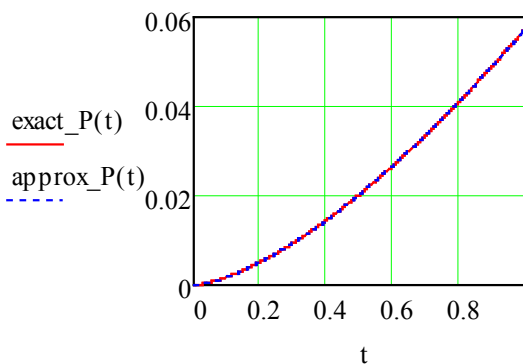

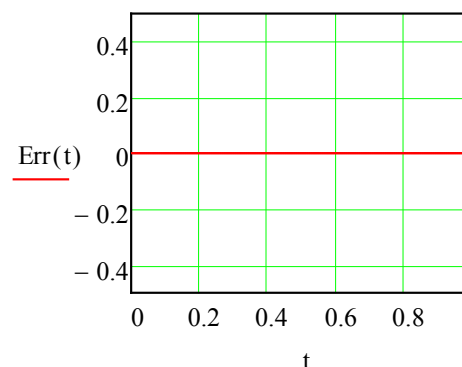**Figure 1** – Graphs of approximate and
exact heat flux functions

Figure 2 – Graph of relative error function

Conclusion

The new method radial heat polynomials is introduced and is used for testing heat process in two phases when heat flux passes through these two zones. The coefficients of temperatures $\theta_1(r,t)$ and $\theta_2(r,t)$ are determined from recurrent formulas (19), (20) and (25), then by using these coefficients and comparing degree of time from condition (3) heat flux is described. To testing effectiveness of radial heat polynomials and integral error function test problem is considered in which free boundaries are represented in self-similar form $\alpha(t) = \alpha_0\sqrt{t}$ and $\beta(t) = \beta_0\sqrt{t}$ which are convenient for testing and with approximation method (collocation method) checked the error estimates between exact solution and approximate solution of this inverse problem.

Acknowledgement

References

1   R. Holm, Electrical Contacts, Fourth Edition, Springer Verlag (198): 482.

2   V.I. Kudrya, A.E. Pudy, S.N. Kharin. Fundamental solution and heat potentials of heat equation for a rod with a variable cross-section. Equations with discontinuous coefficients and their applications, Nauka (1985): 76-81.

3   S.N.Kharin, M.M.Sarsengeldin, H.Nouri. Analytical solution of two phase spherical Stefan problem by heat polynomials and integral error functions. AIP Conference Proceedings 1759, 020031, (2016), doi: http://dx.doi.org/10.1063/1.4959645

4   Alexey A. Kavokin, Targyn A. Nauryz, Nazerke T. Bizhigitova, "Exact solution of two phase spherical Stefan problem with free boundaries", AIP Conference Proceedings 1759, 020117 (2016), https://doi.org/10.1063/1.495931

5   M. M. Sarsengeldin, A. S. Erdogan, T.A. Nauryz, H. Nouri, "An approach for solving an inverse spherical Stefan problem arising in modeling of electrical contact phenomena", *Mathematical Methods in the Applied Sciences* vol. 41, No. 2 (2017): https://doi.org/10.1007/978-3-319-67053-937.

6   M. Sarsengeldin, S. N. Kharin, "Method of the Integral Error Functions for the solution of one- and two-phase Stefan problems and its application", Filomat 31:4 (2017): 1017-1029. DOI 10.2298/FIL1704017S. Available at: http://www.pmf.ni.ac.rs/filomat.

7   Merey M. Sarsengeldin, Targyn A. Nauryz, Nazerke T. Bizhigitova, Alibek M. Orinbasar. Solution of an inverse two phase spherical Stefan test problem. Accepted for publication. Proceedings in Mathematics and Statistics, Springer book series, volume: Functional Analysis in Interdisciplinary Applications (2017).

M.G. Peretyat'kin*, A.A. Kalshabekov

Institute of Mathematics and Mathematical Modeling, Almaty, Kazakhstan
*e-mail: peretyatkin@math.kz

FINITE DOMAIN STRUCTURES IN THE FRAMEWORK OF THE CONCEPT OF A MODEL-THEORETIC PROPERTY

Abstract. In this work, we follow the algebraic approach using definability by formulas presentable in both existential and universal forms. The class of algebraic Cartesian interpretations of theories is studied presenting a foundation of the finitary first-order combinatorics. Common properties of first-order definability in finite models are studied. Some relations are obtained between automorphism groups of finite models and isomorphisms of Cartesian extensions of their theories. A formal definition of the notion of a model-theoretic property is analyzed based on a separate consideration of cases of theories with finite and infinite models. A description of model-theoretic properties defined via finite domains is found. It is established that the class of all finite models with first-order definable elements as well as the corresponding class of theories of such models forms the only model-theoretic property and, therefore, is of little interest as a database with an interface based on the first-order logic language.

Key words: first-order logic, Cartesian extension of a theory, Tarski-Lindenbaum algebra, model-theoretic property, computable isomorphism.

Introduction

We use the radical approach in model theory counting that *model-theoretic properties* are classes of complete theories, cf. [1]. By specification [2], a class $\mathfrak{p}$ of complete theories is a *real model-theoretic property* (corresponding to the common practice of investigations in model theory), if $\mathfrak{p}$ is closed under algebraic isomorphisms of theories as well as under Cartesian extensions and inverse passages in the operation of a Cartesian extension of a theory. A preliminary motivation to the possibility of a formal definition for the concept of a model-theoretic property is considered in [3], while the work [2] describes a final version of this definition. Some applications of the definition of a model-theoretic property are contained in [4].

In this work, structure of real model-theoretic properties is studied based on a separate consideration of the cases of complete theories with finite and infinite models. Based on this, we give an application concerning finite models.

Preliminaries

We consider theories in first-order predicate logic *with equality* and use general concepts of model theory, algorithm theory, constructive models, and Boolean algebras found in [5], [6], and [7]. Special concepts used in the works are defined in [3].

Generally, *incomplete theories* are considered. In the work, the signatures are considered only, which admit Godel's numberings of the formulas. Such a signature is called *enumerable*.

By $L(T)$, we denote the *Tarski-Lindenbaum algebra* of formulas of theory T without free variables, while $\mathcal{L}(T)$ denotes the Tarski-Lindenbaum algebra $L(T)$ considered together with a *Gödel numbering* γ; thereby, the concept of a *computable isomorphism* is applicable to such objects. A finite signature is called *rich*, if it contains at least one n-ary predicate or function symbol for $n \geqslant 2$, or two unary function symbols. By $\mathbb{C}$, we denote the class of all complete theories of enumerable signatures. The record $T \approx S$ means *isomorphism* of theories T and S, while $T \approx_a S$ stands for *algebraic isomorphism* of the theories, cf. [3].

We follow the *algebraic type of definability* using $\exists\bigcap\forall$-formulas affecting more delicate properties of theories in comparison with the normal approach based on the definability via arbitrary first-order formulas. As an $\exists\bigcap\forall$-formula $\varphi(\bar{x})$ of signature σ, we mean a pair of formulas $\left(\varphi^e(\bar{x}), \varphi^a(\bar{x})\right)$ together with the *domain sentence* $DomEA(\varphi(\bar{x})) = (\forall\bar{x})[\varphi^e(\bar{x}) \leftrightarrow \varphi^a(\bar{x})]$, where $\varphi^e(\bar{x})$ is an $\exists$-formula, while $\varphi^a(\bar{x})$ is a $\forall$-formula of signature σ. A formula $\varphi(\bar{x})$ of theory T is said to be $\exists\bigcap\forall$-*presentable* in T if $T \vdash DomEA(\varphi(\bar{x}))$. If $\psi(\bar{x})$ is a

quantifier-free formula, $DomEA\big(\psi(\bar{x})\big)$ is supposed to be a generally true formula. If $\varkappa$ is a finite set (or a sequence) of $\exists\bigcap\forall$-formulas $\psi_i(\bar{x}_i)$, $i < k$, we denote by $DomEA(\varkappa)$ the conjunction $\bigwedge_{i<k} DomEA\big(\psi_i(\bar{x}_i)\big)$.

We formulate a technical statement.

Lemma 0.1. [8, Lemma 2.4.2] *Let $\mathfrak{M}$ be a finite model of an enumerable signature σ. Then, any formula $\varphi(x_1, \dots, x_n)$ of signature σ is equivalent in theory $T = Th(\mathfrak{M})$ to an $\exists\bigcap\forall$-formula of signature σ.*

Proof. By condition, theory T has a unique up to an isomorphism model $\mathfrak{M}$; moreover, $\mathfrak{M}$ is finite. Therefore, any isomorphic embedding of models of theory T is elementary. By Robinson's Criterion, [9], we obtain that theory T is model complete. Hence, we have the $\exists$-reducibility as well as $\forall$-reducibility of any formula in theory T. □

Cartesian-type interpretations

We use a standard concept of an *interpretation* of a theory T_0 in the region $U(x)$ of a theory T_1, [10, Section 4.7]. An interpretation is called *effective* if it is defined by a computable function. Classes of *isostone* and *model-bijective* interpretations are introduced in [11]. In this section, we introduce a technical class of interpretations presenting finitary methods in first-order logic.

Given a signature σ and a finite sequence of formulas of this signature of either of the following forms:

$$\text{(a)} \quad \varkappa = \langle \varphi_1^{m_1} / \varepsilon_1, \varphi_2^{m_2} / \varepsilon_2, \dots, \varphi_s^{m_s} / \varepsilon_s \rangle, \quad (1.1)$$

$$\text{(b)} \quad \varkappa = \langle \varphi_1^{m_1}, \varphi_2^{m_2}, \dots, \varphi_s^{m_s} \rangle,$$

where $\varphi_k(\bar{x}_k)$ is a formula with m_k free variables, $\varepsilon_k(\bar{y}_k, \bar{z}_k)$ is a formula with $2m_k$ free variables such that $Len(\bar{y}_k) = Len(\bar{z}_k) = m_k$; moreover, (1.1)(b) is a simplified notation instead of the common entry (1.1)(a) in the case when $\varepsilon_k(\bar{y}_k, \bar{z}_k)$ coincides with $\bar{y}_k = \bar{z}_k$ for all $k \leqslant s$.

Starting from a model $\mathfrak{M}$ of signature σ together with a tuple $\varkappa$ of any of the forms (1.1)(a,b), we are going to construct a new model $\mathfrak{M}_1$ of signature

$$\sigma_1 = \sigma \cup \{U^1, U_1^1, U_2^1, \dots, U_s^1\} \cup$$

$$\{K_1^{m_1+1}, K_2^{m_2+1}, \dots, K_s^{m_s+1}\} \quad (1.2)$$

as follows. As the universe, we take $|\mathfrak{M}_1| = |\mathfrak{M}| \cup A_1 \cup A_2 \cup \dots \cup A_s$, where all specified parts are

pairwise disjoint sets. On the set $|\mathfrak{M}|$, all symbols of signature σ are defined exactly as they were defined in $\mathfrak{M}$; in the remainder, they are defined trivially; predicate $U(x)$ distinguishes $|\mathfrak{M}|$; predicate $U_k(x)$ distinguishes A_k; the other predicates are defined by specific rules depending on the case. In the case (1.1)(b), each predicate $K_k(\bar{x}_k, u)$ in (1.2) should be defined so that it would represent a one-to-one correspondence between the set of tuples $\{\bar{a} \mid \mathfrak{M} \models \varphi_k(\bar{a})\}$ and the set $A_k = U_k(\mathfrak{M}_1)$. Turn to the most common case (1.1)(a). Denote by $Equiv(\varepsilon_k, \varphi_k)$ a sentence stating that ε_k is an equivalence relation on the set of tuples distinguished by the formula $\varphi_k(\bar{x}_k)$ in $\mathfrak{M}$. In this case, $(m_k + 1)$-ary predicate $K_k(\bar{x}_k, u)$ should be defined so that it would represent a one-to-one correspondence between the quotient set $\{\bar{a} \mid \mathfrak{M} \models \varphi_k(\bar{a})\} / \varepsilon'_k$ and the set $U_k(\mathfrak{M}_1)$, where

$$\varepsilon'_k(\bar{y}_k, \bar{z}_k) = \varepsilon_k(\bar{y}_k, \bar{z}_k) \vee \neg\, Equiv(\varepsilon_k, \varphi_k). \quad (1.3)$$

The model $\mathfrak{M}_1$ obtained from $\mathfrak{M}$ and $\varkappa$ as explained above is denoted by $\mathfrak{M}\langle\varkappa\rangle$.

The aim of replacement of ε_k by ε'_k using $Equiv(\varepsilon_k, \varphi_k)$ is to provide the total definiteness of the operation $(\mathfrak{M}, \varkappa) \mapsto \mathfrak{M}\langle\varkappa\rangle$ independently of whether the formulas ε_k, $k = 1, 2, \dots, s$, represent equivalence relations in corresponding domains or not. In the case (1.1)(a), $\mathfrak{M}\langle\varkappa\rangle$ is said to be a *Cartesian-quotient extension* of $\mathfrak{M}$, while in the case (1.1)(b), the model $\mathfrak{M}\langle\varkappa\rangle$ is said to be a *Cartesian extension* of $\mathfrak{M}$ by a sequence of formulas $\varkappa$.

Mention some kind of determinism for the operation under consideration.

Lemma 1.1. *Given a signature σ and a tuple $\varkappa$ of the form* (1.1)(a). *For a fixed choice of signature* (1.2), *Cartesian-quotient extension $\mathfrak{M}_1 = \mathfrak{M}\langle\varkappa\rangle$ of the model $\mathfrak{M}$ is defined uniquely, up to an isomorphism over $\mathfrak{M}$. Moreover, we have $|\mathfrak{M}_1| = acl\big(U(\mathfrak{M}_1)\big)$. Thus, any automorphism $\lambda\colon \mathfrak{M} \to \mathfrak{M}$ can be extended, by a unique way, up to an automorphism $\lambda^*\colon \mathfrak{M}\langle\varkappa\rangle \to \mathfrak{M}\langle\varkappa\rangle$.*

Proof. This statement is an immediate consequence of the construction. □

Expand the operation of an extension (initially defined for models) on theories. Given a theory T and a tuple $\varkappa$ of the form (1.1). Using a fixed signature (1.2) for extensions of models, we define a new theory $T' = T\langle\varkappa\rangle$ as follows: $T' = Th(K)$, $K = \{\mathfrak{M}\langle\varkappa\rangle \mid \mathfrak{M} \in Mod(T)\}$. In the case (1.1)(a) it is called a *Cartesian-quotient extension* of T, while in the case (1.1)(b) it is called a *Cartesian extension* of T by a sequence $\varkappa$.

We study simple properties of Cartesian-type extensions.

Lemma 1.2. *For any model $\mathfrak{M}$ of theory $T\langle\varkappa\rangle$, there is a model $\mathfrak{N}$ of theory T such that an isomorphism $\mathfrak{M} \cong \mathfrak{N}\langle\varkappa\rangle$ takes place.*

Proof. Immediately, from definition of the operation $T \mapsto T\langle\varkappa\rangle$. □

In theory $T\langle\varkappa\rangle$, the region $U(x)$ represents a model of theory T. Particularly, the transformation $T \mapsto T\langle\varkappa\rangle$ defines a natural interpretation $I_{T,\varkappa}$ of T in $T\langle\varkappa\rangle$. It is called a *plain Cartesian-quotient interpretation*. Similar definition applies to the other case of the tuple $\varkappa$; thereby, the concept of a *plain Cartesian interpretation* is also defined. Considering theories up to an algebraic isomorphism, we may use shorter terms *Cartesian-quotient* or, respectively, *Cartesian* interpretation, for details, cf. [12].

Lemma 1.3. *Given a theory T of an enumerable signature σ and a sequence of formulas $\varkappa$. The plain Cartesian-quotient interpretation $I_{T,\varkappa}: T \mapsto T\langle\varkappa\rangle$ is effective, model-bijective, and isostone. In particular, the interpretation $I_{T,\varkappa}$ determines a computable isomorphism $\mu_{T,\varkappa}: \mathcal{L}(T) \longrightarrow \mathcal{L}(T\langle\varkappa\rangle)$ between the Tarski-Lindenbaum algebras.*

Proof. Immediately. □

Normally, we consider passages $T \mapsto T\langle\varkappa\rangle$ with a sequence (1.1) satisfying the following technical condition:

$$formulas\ \varphi_k(\bar{x}_k)\ and\ \varepsilon_k(\bar{y}_k, \bar{z}_k)\ are \quad \exists\bigcap\forall\text{-}presentable,\ for\ all\ k \leqslant s. \quad (1.4)$$

Denote by $KD(\sigma)$ and $KC(\sigma)$ the sets of tuples of formulas of signature σ of the forms, respectively, (1.1)(a) and (1.1)(b), while KD and KC are unions of these sets for all possible enumerable signatures σ. We denote by $KC_{\exists\bigcap\forall}$ the set of all tuples (1.1)(b) satisfying (1.4), while $KD^{\varepsilon}_{\exists\bigcap\forall}$ is the set of all tuples (1.1)(a) satisfying (1.4). When using an entry $T\langle\varkappa\rangle$, we always suppose that theory T is applicable to the tuple $\varkappa$; moreover, it is supposed that $T \vdash DomEA(\varkappa)$ whenever $\varkappa \in KC_{\exists\bigcap\forall}$ or $\varkappa \in KD^{\varepsilon}_{\exists\bigcap\forall}$.

By applying an extra term *algebraic*, we explicitly indicate that the algebraic approach is accepted. For instance, a passage $T \mapsto T\langle\varkappa\rangle$ is said to be an *algebraic Cartesian-quotient extension* whenever $\varkappa \in KD^{\varepsilon}_{\exists\bigcap\forall}$, an interpretation $I_{T,\varkappa}$ is said to be a *plain algebraic Cartesian interpretation* if $\varkappa \in KC_{\exists\bigcap\forall}$, etc.

We consider combinatorial properties of Cartesian-type extensions.

Lemma 1.4. *Given a theory T of an enumerable signature σ together with a sequence of formulas $\varkappa$. The following statements are satisfied, where all indicated passages are supposed to be effective with respect to Gödel's numbers of tuples of formulas; moreover, the choice of tuples is limited by the condition of applicability to corresponding theories:*

(a) *Suppose that $\varkappa \in KD$. For any $\varkappa'$ in KD, there is a tuple $\varkappa''$ in KD such that an isomorphism*

$$T\langle\varkappa^\wedge\varkappa'\rangle \approx (T\langle\varkappa\rangle)\langle\varkappa''\rangle \quad (1.5)$$

takes place; and vice versa, for any $\varkappa''$ in KD, there is a tuple $\varkappa'$ in KD such that an isomorphism (1.5) takes place.

(b) *Suppose that $\varkappa \in KC$. For any $\varkappa'$ in KC, there is a tuple $\varkappa''$ in KC such that an isomorphism (1.5) takes place; and vice versa, for any $\varkappa''$ in KC, there is a tuple $\varkappa'$ in KC such that an isomorphism (1.5) takes place.*

(c) *Suppose that $\varkappa \in KC_{\exists\bigcap\forall}$. For any $\varkappa'$ in $KC_{\exists\bigcap\forall}$, there is a tuple $\varkappa''$ in $KC_{\exists\bigcap\forall}$ such that an isomorphism*

$$T\langle\varkappa^\wedge\varkappa'\rangle \approx_a (T\langle\varkappa\rangle)\langle\varkappa''\rangle \quad (1.6)$$

takes place; and vice versa, for any $\varkappa''$ in $KC_{\exists\bigcap\forall}$, there is a tuple $\varkappa'$ in $KC_{\exists\bigcap\forall}$ such that an isomorphism (1.6) takes place.

Proof. Validity of these statements can be checked by applying a routine construction based on expressive possibilities of first-order logic. □

Introduce notations for two following relations on the class of arbitrary theories including both complete and incomplete ones:

$$(a)\ T \cong_a S \Leftrightarrow_{dfn}$$
$$(\exists\varkappa'\varkappa'' \in KC_{\exists\bigcap\forall})[T\langle\varkappa'\rangle \approx_a S\langle\varkappa''\rangle], \quad (1.7)$$

$$(b)\quad T \cong_a^\circ S \Leftrightarrow_{dfn}$$
$$\left(\exists\ computable\ isomorphism\ \mu: \mathcal{L}(T) \longrightarrow \mathcal{L}(S)\right)$$

$$(\forall\ complete\ extension\ T' \supseteq T)$$
$$(\forall\ complete\ extension\ S' \supseteq S)$$

$$[S' = \mu(T') \Rightarrow (\exists\varkappa'\varkappa'' \in$$
$$KC_{\exists\bigcap\forall})(T'\langle\varkappa'\rangle \approx_a S'\langle\varkappa''\rangle)].$$

Lemma 1.5. *The relation (1.7)(a) on the class of theories of enumerable signatures is reflexive, symmetric, and transitive (that is, this is an*

equivalence relation). Besides, (1.7)(b) *is also an equivalence relation on the class of all theories. Moreover, we have* $T \cong_a S \Rightarrow T \cong_a^\circ S$ *for all theories T and S, and* $T_1 \cong_a T_2 \Leftrightarrow T_1 \cong_a^\circ T_2$ *for all complete theories T_1 and T_2.*

Proof. Obviously, $\cong_a$ is reflexive and symmetric. Now, suppose that $T \cong_a H$ and $H \cong_a S$ is satisfied. By definition, there are tuples $\xi_i \in KC_{\exists \cap \forall}$, $i = 1,2,3,4$, such that $T\langle \xi_1 \rangle \approx_a H\langle \xi_2 \rangle$ and $H\langle \xi_3 \rangle \approx_a S\langle \xi_4 \rangle$. By applying Lemma 1.4(c), we can find tuples ξ'_2 and ξ'_3 in $KC_{\exists \cap \forall}$ such that the following algebraic isomorphisms take place: $T\langle \xi_1 {}^\wedge \xi'_3 \rangle \approx_a H\langle \xi_2 {}^\wedge \xi_3 \rangle \approx_a H\langle \xi_3 {}^\wedge \xi_2 \rangle \approx_a S\langle \xi_4 {}^\wedge \xi'_2 \rangle$. Thus, we obtain $T \cong_a S$ ensuring the transitivity property. The fact that relation (1.7)(b) is reflexive, symmetric, and transitive on the class of all theories is checked immediately. As for the pointed out links between the relations $\cong_a$ and $\cong_a^\circ$, they are derived based on definitions (1.7)(a) and (1.7)(b) together with properties of the computable isomorphisms μ in Lemma 1.3. □

There are model-type versions $\cong$ and $\cong^\circ$ of the relations without index a, thus, discarding the algebraic mode of definability. For this, we have to use common class KC instead of specialized one $KC_{\exists \cap \forall}$ in the rules (1.7)(a) and (1.7)(b).

Formal specification for a model-theoretic property

We use a general specification to the concept of a *real model-theoretic property*, [2]. By accepting the *pragmatic* approach, cf. Definition 4 and Definition 6 in [2], we have for all complete theories T and S:

$$T \text{ and } S \text{ have identical real} \atop \text{model-theoretic properties } \Leftrightarrow T \cong_a S. \quad (2.1)$$

As for the common rule (1.7)(b), it represents the relation of coincidence of real model-theoretic properties for arbitrary first-order theories (including incomplete ones).

Virtual isomorphisms for finite models

We prove the following fact of a technical character.

Lemma 3.1. [8, Theorem 2.4.4] *Let $\mathfrak{M}$ and $\mathfrak{N}$ be finite models of enumerable signatures such that an isomorphism $Aut(\mathfrak{M}) \cong Aut(\mathfrak{N})$ takes place. Then, we have $Th(\mathfrak{M}) \cong Th(\mathfrak{N})$, i.e., the following relation is satisfied:* $(\exists \varkappa \varkappa' \in KC)[Th(\mathfrak{M})\langle \varkappa \rangle \approx Th(\mathfrak{N})\langle \varkappa' \rangle]$.

Proof. Consider two finite models $\mathfrak{M}$ and $\mathfrak{N}$ whose automorphism groups are isomorphic. Let $T = Th(\mathfrak{M})$ and $S = Th(\mathfrak{N})$. We assume that the universe sets of the models $|\mathfrak{M}| = \{a_1, ..., a_m\}$, $|\mathfrak{N}| = \{b_1, ..., b_n\}$ as well as their signatures τ and σ are disjoint. Fix an isomorphism $q: Aut(\mathfrak{M}) \to Aut(\mathfrak{N})$ and construct a new model $\mathfrak{P}$ of signature $\tau \cup \sigma \cup \{U^1, V^1, R^{m+n}\}$ as follows. We put

$$|\mathfrak{P}| = |\mathfrak{M}| \cup |\mathfrak{N}|,$$

$$U(x) \Leftrightarrow x \in |\mathfrak{M}|, \quad V(x) \Leftrightarrow x \in |\mathfrak{N}|,$$

$$\tau\text{-relations on } |\mathfrak{M}| \text{ are the same as in } \mathfrak{M}, \atop \text{they are trivial in remains,}$$

$$\sigma\text{-relations on } |\mathfrak{N}| \text{ are the same as in } \mathfrak{N}, \atop \text{they are trivial in remains,}$$

$$R = \{\langle \mu(a_1), ..., \mu(a_m), q\mu(b_1), ..., q\mu(b_n) \rangle \mid \mu \in Aut(\mathfrak{M})\}.$$

Due to connections via predicate R, any automorphism of the model $\mathfrak{P}$ acts in coordination on both models $\mathfrak{M}$ and $\mathfrak{N}$. In particular, we have $Aut(\mathfrak{M}) \cong Aut(\mathfrak{P}) \cong Aut(\mathfrak{N})$. Moreover, any automorphism λ of $\mathfrak{P}$ is an identical mapping on the whole model $\mathfrak{P}$ whenever it is identical on $|\mathfrak{M}|$. By Beth's Definability Theorem, [5], all elements in $\mathfrak{P}$ are first-order definable over its domain $U(\mathfrak{P})$. Therefore, the natural interpretation of T in $Th(\mathfrak{P})$ is exact. By Lemma 3.2 in [12], the theory $Th(\mathfrak{P})$ is isomorphic to the theory $T\langle \varkappa' \rangle$ for a sequence $\varkappa' \in KD$. Moreover, Lemma 3.3 in [12] is applicable. Thus, we have $\varkappa' \in KC$. A similar reasoning shows that theory $Th(\mathfrak{P})$ is isomorphic to theory $S\langle \varkappa'' \rangle$ for a sequence $\varkappa'' \in KC$. □

Model-theoretic properties versus finite/infinite models

In this paragraph, we establish how finite models are related with the concept of a real model-theoretic property introduced in [2].

From the rule (2.1) we obtain that the set of all real model-theoretic properties has the form of a complete Boolean algebra of subsets $\mathcal{P}(\mathbb{C}/\cong_a)$. Moreover, separate classes $[T]_{\cong_a}$, $T \in \mathbb{C}$, are *atoms* of this Boolean algebra. They are said to be *atomic model-theoretic properties*.

The following presentation takes place.

Lemma 4.1. *An arbitrary class* $\mathfrak{p}$ *of complete theories is a real model-theoretic property if and only if* $\mathfrak{p}$ *is the union of a family of atomic model-theoretic properties.*

Proof. Immediately. □

Lemma 4.2. *Let* $\mathfrak{M}$ *and* $\mathfrak{N}$ *be abritrary models of enumerable signatures such that* $(\exists \varkappa \varkappa' \in KD)[Th(\mathfrak{M})\langle \varkappa \rangle \approx Th(\mathfrak{N})\langle \varkappa' \rangle]$. *The following assertions are satisfied :*

(a) $\mathfrak{M}$ *is finite if and only if* $\mathfrak{N}$ *is finite,*

(b) $Aut(\mathfrak{M}) \cong Aut(\mathfrak{N})$.

Proof. These statements are provided by construction of a Cartesian-quotient extension of a model, cf. Lemma 1.1 together with Lemma 1.2. □

Let us present the set $\mathbb{C}$ of all complete theories of enumerable signatures in the form $\mathbb{C} = \mathbb{C}_\infty \cup \mathbb{C}_0$, where

$$\mathbb{C}_\infty = \{T \in \mathbb{C} \mid T \text{ has an infinite model}\},$$

$$\mathbb{C}_0 = \{T \in \mathbb{C} \mid T \text{ has a finite model}\}.$$

By definition, we have $KC_{\exists \cap \forall} \subseteq KC \subseteq KD$. Therefore, by Lemma 4.2, each of the sets $\mathbb{C}_\infty$ and $\mathbb{C}_0$ is closed under the equivalence relation $\cong_a$. Thus, any real model-theoretic property $\mathfrak{p} \subseteq \mathbb{C}/\cong_a$ can be decomposed into two parts as follows:

$$\mathfrak{p} = \mathfrak{p}' \cup \mathfrak{p}'', \quad \text{where } \mathfrak{p}'' \subseteq {}^{\mathbb{C}_\infty}/_{\cong_a}$$
$$\text{and } \mathfrak{p}' \subseteq \mathbb{C}_0/\cong_a. \qquad (4.1)$$

Moreover, decomposition (4.1) is defined uniquely for any given property $\mathfrak{p}$.

A model-theoretic property $\mathfrak{p}$ is said to be *purely infinite* if the part $\mathfrak{p}'$ in decomposition (4.1) is empty. The property $\mathfrak{p}$ is said to be *purely finite* if the part $\mathfrak{p}''$ in (4.1) is empty. Obviously, there are properties $\mathfrak{p}$ for which both parts $\mathfrak{p}'$ and $\mathfrak{p}''$ in (4.1) are nonempty. Purely infinite model-theoretic properties are normally considered in traditional model theory. As for the purely finite model-theoretic properties, no regular view on this concept had been available before the definition of a model-theoretic property in the work [2] was appeared.

Lemma 4.3. *Let* $\mathfrak{M}$ *and* $\mathfrak{N}$ *be finite models of enumerable signatures such that* $Aut(\mathfrak{M}) \cong Aut(\mathfrak{N})$. *Then, we have* $(\exists \varkappa \varkappa' \in KC_{\exists \cap \forall})[Th(\mathfrak{M})\langle \varkappa \rangle \approx_a Th(\mathfrak{N})\langle \varkappa' \rangle]$.

Proof. By applying Lemma 3.1 together with Lemma 0.1. □

Theorem 4.4. *Let* $\mathfrak{M}$ *and* $\mathfrak{N}$ *be finite models. The theories* $Th(\mathfrak{M})$ *and* $Th(\mathfrak{N})$ *have identical real model-theoretic properties if and only if their automorphism groups* $Aut(\mathfrak{M})$ *and* $Aut(\mathfrak{N})$ *are isomorphic.*

Proof. Part $\Rightarrow$ is provided by relations (2.1) and (1.7)(a) together with an inclusion $KC_{\exists \cap \forall} \subseteq KD$ and Lemma 4.2. The back implication $\Leftarrow$ is proved from Lemma 4.3 together with relations (1.7)(a) and (2.1).

The following statement characterizes atomic purely finite model-theoretic properties.

Theorem 4.5. *An arbitrary class* $\mathfrak{p}$ *of complete theories is an atomic purely finite model-theoretic property if and only if the following is satisfied for a finite group* G:

$$p = p_G =_{dfn} \{Th(\mathfrak{M}) \mid \mathfrak{M} \in FinMod \ \& \ Aut(\mathfrak{M}) \cong G\},$$

where $FinMod$ *is the class of all finite models of enumerable signatures.*

Proof. By applying Theorem 4.4. □

Conclusion

We used a general specification of the concept of a model-theoretic property introduced in [2]. Based on separate analysis of cases for finite and infinite models, we characterize the structure of real model-theoretic properties.

Statements of Theorem 4.4 and Theorem 4.5 fully characterize the case of model-theoretic properties for complete theories with finite models. It is a simple fact that elements in a finite model with the trivial automorphism group are uniquely defined. Thus, such models as well as their theories can be considered as a basis for constructing abstract databases in applied logic. By Theorem 4.5, all models of this class form the only model-theoretic property; i.e., they are not distinguishable from the point of view of model theory. Thereby, it is possible to conclude that the class of all finite models with unique elements as well as the corresponding class of complete theories is not of interest as a database with an interface based on the first-order logic language.

Acknowledgment

References

1   Peretyat'kin M.G. "Hanf's isomorphisms between predicate calculi of finite rich signatures preserving all real model-theoretic properties."

International conference on algebra and logic Maltsev's Meeting, Russia, Novosibirsk, 19-23 August (2019): 202.

2   Peretyat'kin M.G. "First-order combinatorics and a definition to the concept of a model-theoretic property with demonstration of possible applications." Algebra and Model Theory 11, Proceedings of 12-th International Summer School-Conference "Problems Allied to Universal Algebra and Model Theory," Erlagol-2017, June 23-29 (2017): 86-101.

3   Peretyat'kin M.G. "First-order combinatorics and model-theoretic properties that can be distinct for mutually interpretable theories." Siberian Advances in Mathematics, 26(3) (2016): 196-214.

4   Kudaibergenov K.Zh. "On model-theoretical properties in the sense of Peretyat'kin, o-minimality, and mutually interpretable theories." Мат.труды. 26(3) (2016): 190-195.

5   Hodges W. "A shorter model theory." Cambridge University Press, Cambridge (1997).

6   Rogers H.J. "Theory of Recursive Functions and Effective Computability." Mc. Graw-Hill Book Co., New York (1967).

7   Ershov Yu.L and Goncharov S.S. "Constructive models." Transl. from the Russian. (English) Siberian School of Algebra and Logic. New York, NY: Consultants Bureau. XII (2000).

8   Peretyat'kin M.G. "Finitely axiomatizable theories and similarity relations." *American Math. Soc. Transl.*, 195(2) (1999): (309-346).

9   Robinson A. "Introduction to model theory and to the metamathematics of algebra." North-Holland, Amsterdam (1963).

10   Shoenfield J.R. "Mathematical Logic." Addison-Wesley, Massachusetts (1967).

11   Peretyat'kin M.G. "Finitely axiomatizable theories." Plenum, New York (1997).

12   12. Peretyat'kin M.G. "A technical prototype of the finite signature reduction procedure for the algebraic mode of definability." *Kazakh Mathematical Journal*, 19(2) (2019): 78-104.

F.F. Komarov[1], T.A. Shmygaleva[2*] ,
A.A. Kuatbayeva[3], A.A Srazhdinova[2]

[1]Belarusian State University, Minsk, Belarus
[2]al-Farabi KazNU, Kazakhstan, Almaty
[3]IITU, Kazakhstan, Almaty
*e-mail: shmyg1953@mail.ru

COMPUTER SIMULATION OF VACANCY CLUSTERS CONCENTRATION IN TITANIUM IRRADIATED WITH IONS

Abstract. The process of irradiation of metals with ions is an effective method for changing various properties of materials, in particular titanium, as well as obtaining new materials. This work is devoted to modeling radiation processes in titanium irradiated with ions. Algorithms of cascade-probabilistic functions (CPF) computation depending on the number of interactions and the particle penetration deep number for various incident particles of the Mendeleev's periodic table in titanium are presented. Approximate value expressions for cross-sections are chosen, patterns of cooperation cross-sections demeanor, CP-functions depending on observation profound, number of interactions, target atomic number, primary particle initial energy are noted. Algorithms for calculating the radiation imperfections concentration in ion radiation have been developed and computations in titanium in ion radiation have been carried out. With the calculating CPF and the depth distribution of vacancy clusters, it is necessary to find the region of the result in which these characteristics of the process of formation of radiation defects in solids are exists. Regularities obtained when finding this area are formulated. The calculation results in the form of graphs and tables are presented.

Keywords: Modeling, algorithm, computation, ion, regularities, approximate value, CPF, cooperation cross-section, concentration, vacancy accumulations.

Introduction

For metals, ion irradiation is an effective method to alter properties such as metal durability, staining sustainability, weariness, deterioration, etc. At present, radiation physics makes a considerable investment to the development of nanophysics and its related application field - nanoelectronics.

In contradistinction to protons, α-particles, and electrons, (with energy > 1 MeV), Ion particles are able to form cascading regions (vacancy accumulations and accumulations of inter-node atoms). In contradistinction to protons, electrons, and α-particles process of interplay of ions with substance and their passing through substance is heavier task as during creature of physical and mathematical models [1-3]. This can be explained by the specific behavior of ions, for which the calculation of CPF, PVA spectra, the concentration of vacancy clusters, and the selection of approximations produce many features that are eliminated in some way. Furthermore, with the aid of a definite diversity of flyable particles in a particular material it is possible to constitute a predefined structure and chemical compounds enough stable in a wide temperature range [4]. Then the physical and chemical properties of these materials will change. Therefore, when studying the process of ion irradiation of materials, it is necessary to consider and solve a block of physical and mathematical problems. Many papers have been devoted to the study of the interaction of particles with matter and the formation of vacancy clusters under ion irradiation [5]. The primary part of working in this directing is executed within the cascade probability way framework [6].

Main results

The probability of transition in n steps for ions is written as follows [1]:

$$\psi_n(h',h,E_0) = \frac{1}{n!\,\lambda_0{}^n}\left(\frac{E_0-kh'}{E_0-kh}\right)^{-l}\exp\left(\frac{h-h'}{\lambda_0}\right)*\left[\frac{\ln\left(\dfrac{E_0-kh'}{E_0-kh}\right)}{ak}-(h-h')\right]^n,\qquad(1)$$

where n – number of cooperation, h', h – Ion generation and registration deep, σ_0, a, E_0, k – approximate value factors related to cooperation mileage and specific energy loss factor, $\lambda_0 = 1/\sigma_0$.

Cooperation of cross-sections was calculated according to the Reserford formula [1], deep of observations were based on spreadsheets of parameters of spatial allocation of ion-implanted admixture [7]. For ions forming primary- embossed atoms, the dependency of the approximate value function on energy, which in turn depends on the profound of penetration, is represented as follows [1]:

$$\sigma(h) = \sigma_0\left(\frac{1}{a(E_0-kh)}-1\right),\qquad(2)$$

Approximating curve dependencies of σ on h are given in figure 1 and in table 1. Agreement of approximate value and reference curves is very good.
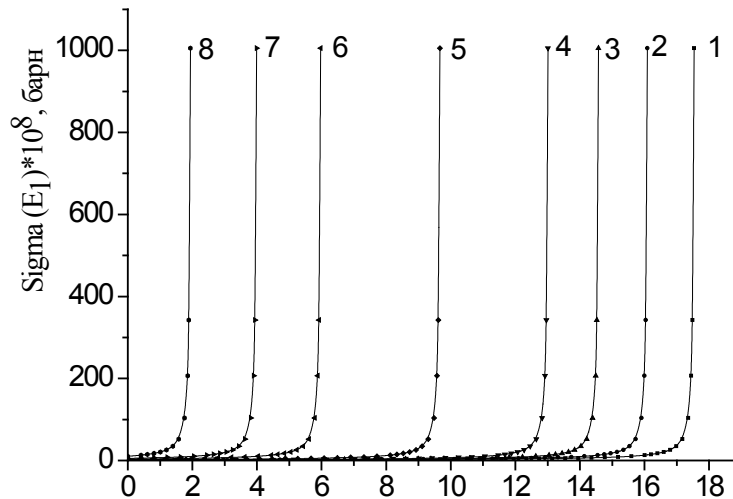

Figure 1 – Approximate value of modified section of CPF for aluminium in titanium E_0 = 1000 (1), 900 (2), 800 (3), 700 (4), 500 (5), 300 (6), 200 (7), and 100 (8) keV. Points - Design Section Deep Dependency Data, Solid Line – Approximate value

Analysis of the computations shows that the approximate value curves of the modified cooperation cross-sections are well described by formula (2), which makes it possible to calculate the CP-functions for aluminum in titanium with high precision. The theoretical correlation ratio ranges from 0, 99 to 0.999.

CPF computations were performed according to formula (1). All computations were made with double accuracy throughout the observation profound interval. The outcomes of the computations show that CPF, depending on h and on n, have the following demeanor: increase, reach the maximum, then decrease. The figures show the relationship of the aluminum CPF in titanium to the number of cooperation (Figures 2, 3) and penetration profound. (Figures 4.5).

At CPF computation on computer depending on interplays number the following regularities arise:

1. Withal increase in atomic heft of the flyable particle the outcome finding area is displaced to the area of small deeps concerning h/λ and narrowed.

2. Withal a huge atomic heft of the flyable particle the CP-function maximum value is showed

to the square of small deeps concerning h/λ already with little deeps, and with huge profounds the outcome is in particularistic area (less than 1%, silver, gold). The narrowest region of the outcome is acquired with a big atomic heft of the flyable particle and a tiny target at the end of the run and achieves hundreds of percent [8, 9]. The computation outcomes are given in Table 2.

Table 1 – Approximate value parameters for aluminum in titanium

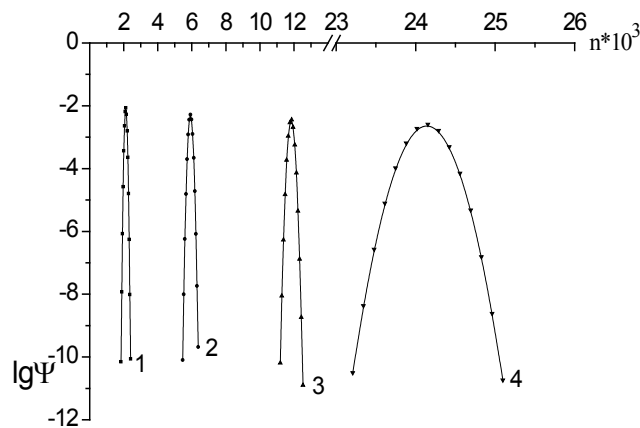| E_0	σ_0*10^8	a	E_0	k	η
1000	0.26338	0.2825	0.67741	385.67808	0.99932
900	0.29435	0.22033	0.6491	402.34914	0.98702
800	0.43114	0.18618	919318,00	987.37947	0.99942
700	0.40218	0.19447	0.67386	512.83839	0.99391
500	0.43023	0.19061	0.65982	677.91892	0.98702
300	0.66686	0.2023	0.83022	1384.2892	0.99944
200	0.56167	0.15111	0.62701	1562.21507	0.9994
100	0.81173	0.10855	0.61751	3138.50145	0.99937

Figure 2 – CPF 's dependency on the interplays number for aluminum in titanium
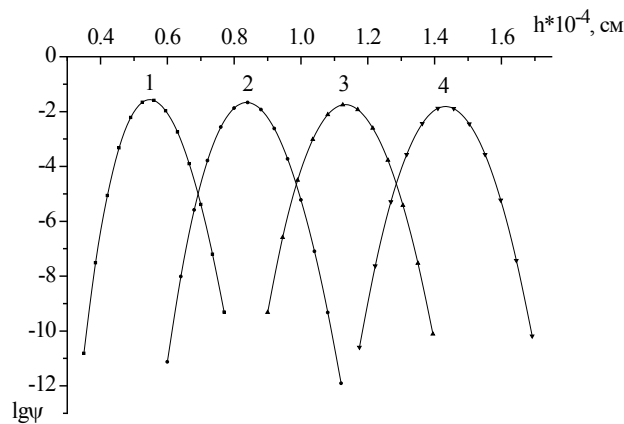at h = 1,5,9,13,17 (* 10^{-4}) cm; E_0 = 1000 keV (1-4)

Figure 3 – Ratio of CPF for titanium carbon at
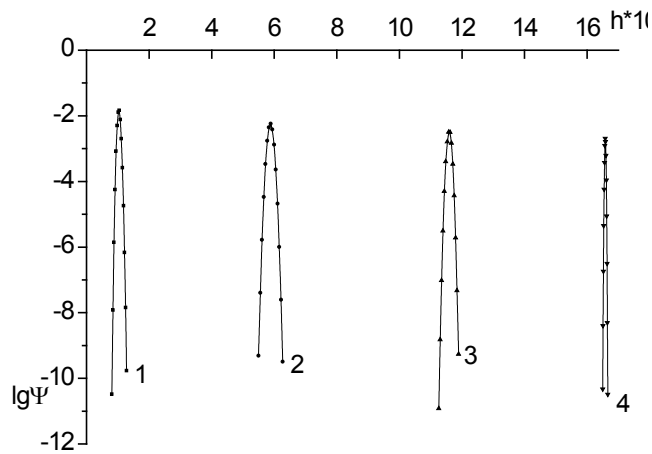deep at E_0 = 300 keV, n= 215; 347; 498; 673 (1-4)

Figure 4 – Dependency ψ_n $(h', h_{,0})E$ from deep for aluminum in titanium
at $E_0 = 1000$ keV for $n = 677; 4704; 13054; 37124$ (1-4)

Table 2 – Left and Right Region Offset Percent Dependency. Outcome from the number of interplays for aluminum in titanium at $E_0 = 1000$ keV

$h * 10^4$, cm	B_1,%	B_2,%	N_n	B_3,%
1	26,23	24	23	50,23
3	22,4	2	40	24,4
5	26,2	-8,7	55	17,5
7	32	-20	65	12
9	39	-30.5	78	8.5
11	47,5	-41,2	95	6,3
13	57,6	-53,2	110	4,4
15	70,3	-67,8	135	2,5
17	89,58	-88,96	165	0,62

Similar patterns were revealed in CPF computations depending on penetration deep with the difference that the area of finding the outcome is shifted to the area of greater deeps [9]. The outcomes of the computations are shown in Table 3.

Table 3 – The percent movement of the left, right edges of the outcome area depends on the penetration deep for titanium aluminum at $E_0 = 1000$ keV

$h*10^4$, cm	h/λ, cm	C_1,%	C_2,%	N_h	C_3,%
1	677	19	31	24	50
3	2373	1	25	60	26
5	4704	-10	26	100	16
7	8031	-18,2	29,8	150	11,6
9	13054	-25,1	32,2	250	7,1
11	21325	-28,9	33	470	4,1
13	37124	-26,9	28,25	470	1,35

Computation of radiation imperfection concentration in case of ion radiation is performed by formula [10]:

$$C_k(E_0, h) = \int_{E_c}^{E_{2\,max}} W(E_0, E_2, h) dE_2 , \qquad (3)$$

E_2 – energy of the primary beaten-out atom, E_{2max} – Maximum kinetic energy the atom will receive, E_c – threshold energy, $W(E_0, E_2, h)$ – spectrum of primary - embossed atoms.

Finding the region of the outcome of the concentration of vacancy accumulations in ion radiation revealed the following patterns:

1. As the atomic number of the flyable particle increases, the range of the outcome region is significantly shifted to the region of greater depths and magnifications, the concentration value at the maximum dot and the concentration values themselves are extremely enlarged.

2. With a huge atomic heft of the flyable particle, the counting time is greatly increased.

3. Depending on the deep of permeation, the elementary and final values of the number of cooperation is increasing, the interval of the outcome square (n0 n1) also increases and changes to the greater profound area.

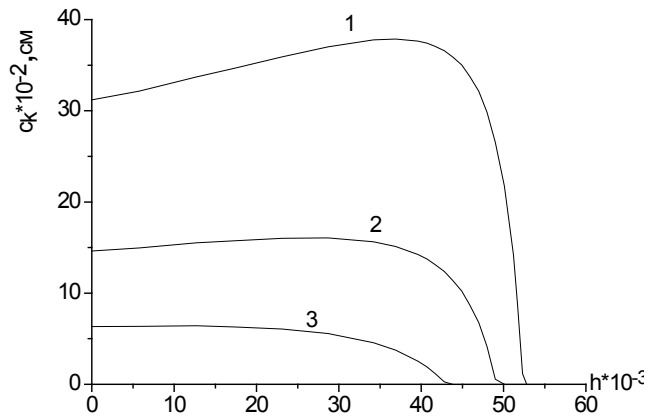The computations outcomes are given in Figures 6.7 and Table 4.

Figure 5 – Dependency of vacancy accumulations concentration on deep of titanium radiation with carbon ions at E_0=800 keV, E_c=50 keV (1), 100 keV (2), 200 keV (3)
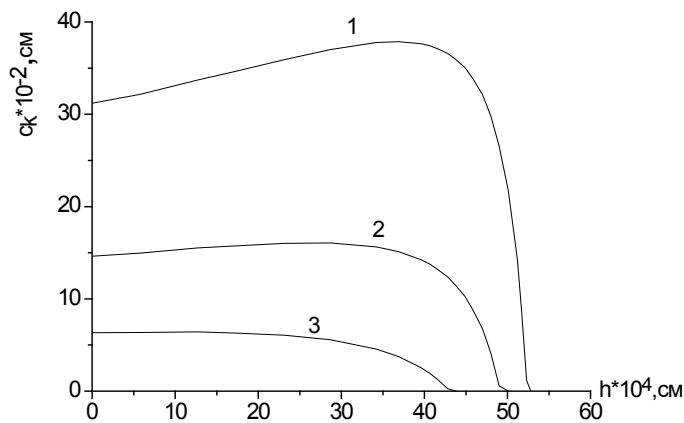

Figure 6 – Dependency of vacancy accumulation concentration on deep of ion radiation for silver in titanium at E_0= 1000, E_c= 50 (1), 100 (2), 200 (3) keV

Table 4 - Limits of the radiation imperfections concentration determination area for silver in titanium at E_c=100 keV, E_0= 1000 keV

h*10 ^{4}, cm	$C_к$, cm^{-1}	E_0, keV	n_0	n_1	τ
0,01	1462,93	1000	0	25	2″
0,58	1495,87	900	196	444	3″
1,27	1552,12	800	546	925	4″
1,74	1575,49	700	809	1253	5″
2,31	1601,31	600	1152	1669	7″
2,87	1604,77	500	1512	2095	9″
3,42	1563,53	400	1900	2539	14″
3,69	1511,67	350	2083	2765	16″
3,96	1424,11	300	2284	2990	17″
4,07	1374,71	280	2367	3090	20″
4,17	1312,41	260	2444	3174	29″
4,28	1237,09	240	2530	3274	31″
4,38	1141,89	220	2609	3363	31″
4,49	1023,67	200	2697	3466	33″
4,59	871,74	180	2778	3563	23″
4,70	675,75	160	2868	3656	23″
4,80	414,37	140	2951	3747	24″
4,90	56,05	120	3035	3847	25″
5,01	0	100	3129	3948	26″

Conclusion

Thus, the work represents mathematical models of cascade-probabilistic functions with considering energy losses for ions, an approximate value expression for the cooperation cross-sections calculated from the Reserford formula. Based on the models obtained, vacancy accumulation concentration models were obtained. Approximate value expression was chosen and approximate value coefficients were found for different flyable particles in titanium. Computations of CPF are performed depending on cooperation number and particle penetration depth for flyable ions in titanium. The demeanor patterns in the outcome area are shown. The vacancy accumulations concentration has been calculated. Patterns of finding the region at the vacancy accumulations concentration outcome for various flyable particles and target titanium have been revealed.

References

1. E.G. Boos, A.A. Kupchishin, A.I. Kupchishin, E.V. Shmygalev, T.A. Shmygaleva. *Cascade and probabilistic method, solution of radiation and physical tasks, Boltzmann's equations. Communication with Markov's chains*. - Monograph. Almaty: KazNPU after Abay, Scien. Res. Inst. for New Chem. Techn. and Mat. under al-Farabi KazNU (2015).

2. Zinovieva A.F, Zinovyev, V.A., Nenashev, A. V., Zhivulko, V., Mudryi, A. "Photoluminescene of compact GtSi quantum dot groups with increased probability of finding and electron in Ge." *Scien. Rep.* 10 (2020).

3. Sahul, M., Smyrnova, K., Harsani M, Babincova, P., Vopat, T. "Effect of lanthanum addition on the struture evolution and mechanical properties of the nanocomposite Ti-Si-N coatings." *Mat. Let.* 276 (2020).

4. Kodanova, S.K., Issanova, M.K., Ramazanov T.S., Khikmetov, A.K., Maiorov, S.A. "Simu;ation of positronium plasma by the molecular dynamics method." *Contr. to Pl. Phys.* 59 (2019).

5. Kozhamkulov, B.A., Akitaj, E., Dzumadillaev, K.N., Primkulova, Z.E., Kyrykbaeva, A.A. "Destruction of Silicon – Organic Composites Irradiated by High-Energy Electrons." *Mech. of Comp. Mat.* 55 (2019): 637-642.

6. Pak, V.K., Ghyngazov, S.A., Miklin, M.B., Lysenko, E.N., Kupchishin A.I. "Hole localization in Thallium Nitrate (I)." *Rus. Phys. J.* 62 (2019): 756-762.

7. Voronova, N.A., Kupchishin A.I., Niyazov, M.N., Taipova, B.G., Abdukhairova, A.T. "Research of electron irradiation effects upon plexigals strain

during bending test." *IOP Conf. S.: Mat. Scien. and Eng.* 289 (2018).

8. Kozhamkulov, B.A., Kupchishin A.I., Bitibaeva, Z. M., V.P. "Radiation-Induced Defect in Composite Materials and Their Destruction Under Electron Irradiation." *Mech. of Comp. Mat.* 53 (2017): 59-64.

9. Voronova N.A., Kupchishin, A.I., Kupchishin, A.A., Kuatbayeva A.A., Shmygaleva, T.A. "Computer Modeling of Vacancy Nanoclusters Depth Distribution in Ion-Irradiated Materials." *K. Engin. Mat.*769 (2018): 358-363.

10. Anatoliy Kupchishin, Nataliya Voronova, Tatyana Shmygaleva, and Alexander Kupchishin. Computer Simulation of Vacancy Clusters Distribution by Depth in Molybdenum Irradiated by Alpha Particles. *K. Engin. Mat.* 781 (2018): 372.

Z.Yu. Fazullin[1] , Zh. Madibaiuly[2*], L. Yermekkyzy[2]

[1]Bashkir State University, Ufa, Russia,
[2]A.Dzholdasbekov Institute of Mechanics and Engineering SC MES RK, Almaty, Kazakhstan
*e-mail: zhumabaymadibaiuly@gmail.com

CONTROL OF VIBRATIONS
OF ELASTICALLY FIXED OBJECTS USING
ANALYSIS OF EIGENFREQUENCIES

Abstract. In this paper, a mathematical model of a controlled system is investigated, created on the basis of a fourth-order differential equation widely used in various fields of science and technology. The problem of managing the behavior of structural elements has been solved. The mechanism of transition from one system to another is considered using the analysis of natural frequencies. The rod can be fixed in different ways (termination, hinge locking, elastic termination, floating termination, free end) [1]. If the ends of the rod are fixed so that resonant vibration frequencies are generated, then the question arises: is it possible to change the fastening of the rod so as to indicate a safe range for controlling the natural frequencies. The question posed by us gives rise to many others, more specific. For example, is it possible to determine how the ends of the bar are fixed by the natural vibration frequencies of the bar? Are they springs, sealed or loose? Such applications are very important especially when the first natural frequency generates a resonance situation. It is necessary to control the natural frequencies so that the system does not receive the first natural frequency for safe operation. The main result is formulated as a theorem. The stress-strain state (SSS) control has been developed for rods with elastic fastening on the left and hinged on the right. The uniqueness theorem for boundary conditions is proved using the analysis of natural frequencies.
Key words: elastically fixed objects, natural frequencies, spectral problem.

Introduction

During the construction of technical structures, along with strength management, the issues of stress-strain state (SSS) management of its individual key elements are also important [7], [2], [8], [9]. These controls significantly affect the technical condition of the entire structure. In this paper, we have developed a SSS control for bars with elastic fixing on the left and hinged on the right. These systems are used in bridge and aircraft structures as parts of superstructure beams and floor slabs. Since the control of SSS is influenced by the natural frequencies of vibrations of the rods, in this work the methods of perturbation of the spectral theory of differential operators [3], [4-5] are used.

The need to calculate natural frequencies and the corresponding vibration modes often arises when analyzing the dynamic behavior of a structure under the influence of variable loads. The most common situation is when, when designing, it is required to make sure that there is a low probability of occurrence of such a mechanical phenomenon as resonance under operating conditions. As you know, the essence of resonance is in a significant (tens of times or more) amplification of the amplitudes of forced oscillations at certain frequencies of external influences – the so-called resonance frequencies. In most cases, the occurrence of resonance is extremely undesirable in terms of ensuring product reliability. A multiple increase in vibration amplitudes at resonance and the resulting high stress levels are one of the main reasons for the failure of products operated under vibration loads. To protect against resonance influences, you can use various mechanical devices that fundamentally change the spectral characteristics of the structure and absorb vibration energy (for example, vibration isolators). However, there is another effective way to counter resonances. It is known that resonances are observed at frequencies close to the frequencies of natural vibrations of the structure. If, when designing a product, it is possible to estimate the spectrum of natural frequencies of a structure, then it is possible with a significant degree of probability to predict the risk of resonances in a known frequency range of external influences. In order to avoid or to significantly reduce the likelihood of resonances, it

is necessary that most of the lower natural frequencies of the structure do not lie in the frequency range of external influences.

Statement of the problem

We put the inverse to this spectral problem: the problem of the natural frequencies of the bending vibrations of the bar to find the unknown boundary conditions: $U_1(y) = 0$, $U_2(y) = 0$. Denote the matrix composed of the coefficients a_{ij} of the forms $U_1(y)$ and $U_2(y)$ through A and its second-order minors – through M_{ij}:

$$A = \begin{Vmatrix} a_{11} & a_{12} & a_{13} & a_{14} \\ a_{21} & a_{22} & a_{23} & a_{24} \end{Vmatrix},$$

$$M_{ij} = \begin{vmatrix} a_{1i} & a_{1j} \\ a_{2i} & a_{2j} \end{vmatrix}.$$

Finding forms $U_1(y)$, $U_2(y)$ is equivalent to finding the matrix A up to linear equivalence . The rod can be fixed in different ways (termination, hinge locking, elastic termination, floating termination, free end) [1].

There are various known cases of fixing the end of the rod. [13,14]

Rigid pinching
$$A = \begin{Vmatrix} 1 & 0 & 0 & 0 \\ 0 & 1 & 0 & 0 \end{Vmatrix};$$

Free support
$$A = \begin{Vmatrix} 1 & 0 & 0 & 0 \\ 0 & 0 & 1 & 0 \end{Vmatrix};$$

Free end,
$$A = \begin{Vmatrix} 1 & 0 & 0 & 1 \\ 0 & 1 & 1 & 0 \end{Vmatrix};$$

Floating termination,
$$A = \begin{Vmatrix} 0 & 1 & 0 & 0 \\ 0 & 0 & 0 & 1 \end{Vmatrix};$$

Five different types of elastic fastening:
$$A = \begin{Vmatrix} c_1 & 0 & 0 & 1 \\ 0 & 1 & 0 & 0 \end{Vmatrix}, \begin{Vmatrix} 1 & 0 & 0 & 0 \\ 0 & -c_2 & 1 & 0 \end{Vmatrix},$$

$$\begin{Vmatrix} c_1 & 0 & 0 & 1 \\ 0 & 0 & 1 & 0 \end{Vmatrix}, \begin{Vmatrix} 0 & 0 & 0 & 1 \\ 0 & -c_2 & 1 & 0 \end{Vmatrix},$$

$$\begin{Vmatrix} c_1 & 0 & 0 & 1 \\ 0 & -c_2 & 1 & 0 \end{Vmatrix}$$

If the ends of the rod are fixed in such a way that resonant vibration frequencies are generated, then the question arises: is it possible to change the fastening of the rod so as to indicate a safe range for controlling natural frequencies.

Before presenting the main results, we recall that the equation of bending vibrations of a homogeneous rod of length l at $0 < x < l$, $t > 0$ with constant bending stiffness has the form

$$\rho A \frac{\partial^2 w(x,t)}{\partial t^2} + EJ \frac{\partial^4 w(x,t)}{\partial x^4} = 0,$$

where $w(x, t)$ – deflection of the current point of the bar axis; ρ – material density; A – cross-sectional area; EJ – bending stiffness of the bar.

We denote $\lambda = \dfrac{\omega^2 \rho A}{EJ}$ As known [14], the frequency of bending vibrations of the beam does not depend on the initial shape of the beam, but depends only on the method of fixing its ends. In the new notation, the problem of bending vibrations of a bar with elastic fixation on the left and hinge on the right by replacement $w(x,t) = y(x)\sin(\omega t)$ reduces to the following spectral problem:

$$y^{IV}(x) = \lambda y(x), \; 0 < x < l, \qquad (1.1)$$

$$c_1 y(x)\big|_{x=0} = y'''(x)\big|_{x=0},$$
$$y(x)\big|_{x=l} = 0,$$
$$y''(x)\big|_{x=0} = 0, \; y''(x)\big|_{x=l} = 0. \quad (1.2)$$

Here c_1 spring coefficient of elasticity.

The operator corresponding to problem (1.1) – (1.2) is denoted by $Ky(x) = \lambda y(x)$. Operator eigenvalues K can be numbered in non-decreasing order

$$\lambda_1 \le \lambda_2 \le \lambda_3 \le \dots$$

Smallest eigenvalue λ_1 is positive, which we will show below. Moreover, the choice of the coefficient of elasticity of the spring significantly affects the behavior of natural frequencies. The system of eigenfunctions $\{y_n(x)\}_{n=1}^{\infty}$ operator K forms an orthonormal basis of the space $L_2(0,l)$.

Problem 1.1: Consider the spectral problem of the operator B corresponding to the following problem:

$$u^{IV}(x) = \mu u(x),\ 0 < x < l, \qquad (1.3)$$

$$c_1 u(x)\big|_{x=0} = u'''(x)\big|_{x=0} + \alpha \int_0^l u(x) y_1(x) dx,$$

$$u(x)\big|_{x=l} = 0,\ u''(x)\big|_{x=0} = 0,\ u''(x)\big|_{x=l} = 0. \ (1.4)$$

Here $y_1(x)$ – the first eigenfunction of the operator K. The boundary parameter α can take complex values.

Select parameter α so that the eigenvalues of the operator B was out of range $(-\lambda_2, \lambda_2)$.

Operator B can be considered a perturbation of the operator K, since only the scope has changed $D(K)$ operator K. Such applications are very important especially when the first natural frequency generates a resonance situation. Another can formulate this problem as follows: It is necessary to control natural frequencies so that the system does not receive the first natural frequency for safe operation. Let us state the main result as a theorem.

Theorem 1.1. If you choose α so that the inequality

$$\lambda_2 - \lambda_1 < \frac{\alpha}{c_1} y_1''(0) \qquad (1.5)$$

then the eigenvalues $\{\mu_n\}_{n=1}^{\infty}$ operator B determined by the formula $\mu_n = \lambda_n$ at $n \geq 2$ and μ_1 is the only real root of the equation $c_1 = \dfrac{\alpha y_1'''(0)}{\mu - \lambda_1}$.

To prove the theorem, we need the following lemma.

Lemma 1.1. Identity is valid

$$(\mu - \lambda_1) \int_0^l u(x) y_1(x) dx =$$

$$= \left(-\frac{1}{c_1} u'''(0) + u(0)\right) y_1'''(0)$$

Proof of Lemma 1.1. The right side of the identity can be written in the following form

$$(\mu - \lambda_1) \int_0^l u(x) y_1(x) dx =$$

$$= \int_0^l \mu u(x) y_1(x) dx - \int_0^l u(x) \lambda_1 y_1(x) dx =$$

$$= \int_0^l u^{IV}(x) y_1(x) dx - \int_0^l u(x) y_1^{IV}(x) dx.$$

Direct calculation shows that the first term is equal to

$$\int_0^l u^{IV}(x) y_1(x) dx =$$

$$= \left(-\frac{1}{c_1} u'''(0) + u(0)\right) y_1'''(0) + \int_0^l u(x) y_1^{IV}(x) dx.$$

Taking into account the last relation, we obtain the proof of Lemma 1.1.

Lemma 1.1 is proved

2. Proof of the theorem 1.1

To prove the theorem, the perturbed boundary condition, taking into account Lemma 1.1, can be written in the following form

$$(c_1 u(0) - u'''(0)) =$$
$$= \frac{\alpha y_1'''(0)}{c_1 (\mu - \lambda_1)} (c_1 u(0) - u'''(0)) \qquad (1.6)$$

By assumption λ_1 is not an eigenvalue of the problem (1.3)- (1.4). Therefore $c_1 u(0) \neq u'''(0)$.

Whence it follows that $c_1 = \dfrac{\alpha y_1'''(0)}{\mu - \lambda_1}$.

Let be $\eta_1 = \lambda_1 + \dfrac{\alpha}{c_1} y_1'''(0)$ и $\dfrac{\alpha}{c_"} y_1'''(0) > \lambda_2 - \lambda_1$.

Then $\eta_1 > \lambda_2$.

Let us calculate the characteristic determinant [6] of the operator B.

Let us calculate the characteristic determinant [6] of the operator K determined by the formula

$$\Delta(\lambda) = 2\cos\left(\sqrt[4]{\lambda}l\right)\cosh\left(\sqrt[4]{\lambda}l\right) -$$
$$- \frac{c_1}{\sqrt[4]{\lambda^3}}\left(\sin\left(\sqrt[4]{\lambda}l\right)\cosh\left(\sqrt[4]{\lambda}l\right) - \cos\left(\sqrt[4]{\lambda}l\right)\sinh\left(\sqrt[4]{\lambda}l\right)\right)$$

At $c_1 = 0$ The characteristic determinant was cleared in detail in [6].

For different values graphic way possible to ensure that the smallest eigenvalue λ_1 is positive.. From relations (1.6) it follows that the perturbed boundary condition takes the form

$$f(\mu)\left(c_1 u(0) - u'''(0)\right) = 0,$$

where $f(\mu) = 1 - \dfrac{\alpha y_1'''(0)}{c_1(\mu - \lambda_1)}$.

Taking into account the last relations, we calculate the explicit form of the characteristic determinant of the operator B

$$\Delta(\mu) = f(\mu)\Delta_0(\lambda).$$

where Δ_0 characteristic determinant of the operator K.

The last representation implies the proof of the theorem.

Conclusion

The study of inverse problems in the spectral theory of differential operators dates back to the fundamental works of the twenties and forties of the twentieth century. The impetus for the development of this direction was the work of V.A. Amburtzumyan and G. Borg. A significant contribution to the formation of this direction was made by A.N. Tikhonov, M.I. Gelfand, N. Levinson, M.G. Crane, B.M. Levitan, V.A. Marchenko, M.G. Gasimov, V.A. Sadovnichy, V.A. Yurko, Gladwell G.M.L. other. In the works of these authors, the coefficients of the boundary conditions (and not all) were identified from the spectra only incidentally with the coefficients of the differential equations themselves. In this case, not one, but two or more spectra, or a spectrum and additionally other spectral data, were used for identification.

In this paper, a mathematical model of a controlled system is investigated, created on the basis of a fourth-order differential equation widely used in various fields of science and technology. The problem of managing the behavior of structural elements has been solved. The mechanism of transition from one system to another is considered using the analysis of natural frequencies.

Also, in this work, the SSS control is developed for rods with elastic fastening on the left and hinged on the right. These systems are used in bridge and aircraft structures as parts of superstructure beams and floor slabs. Since the control of SSS is influenced by the natural frequencies of vibrations of the rods, in this work we use the methods of perturbation of the spectral theory of differential operators.

References

1   Akhtyamov A.M. The theory of identification of boundary conditions and its applications. Moscow: Fizmatlit (2009): 272.
2   Vibration in technology: A Handbook. T. 1. Ed. V.V. Bolotina. – M .: Mechanical Engineering (1978): 352.
3   Kanguzhin B.E., Aniyarov A.A. Well-posed problems for the Laplace operator in a punctured region // *Matem. notes*. Vol. 86, No. 6 (2011): 856-867.
4   Andreev Yu.N. Control of finite-dimensional linear objects, Moscow: Nauka (1976).
5   Islamov G.G. Extremal perturbations of closed operators, Izv. universities. Mat. No. 1 (1989): 35–41.
6   Naimark M.A. Linear differential operators. – Moscow: Nauka (1969): 526.
7   Strett J.W. (Lord Rayleigh). Sound theory. T. 1 – M .; L .: Gostekhizdat (1940).
8   Komkov V. Theory of optimal control of vibration damping of simple elastic systems. – M .: Mir (1975).
9   Kovyryagin M.A., Nikulin S.V., Ovchinnikov I.G. The problem of synthesis of the controller of the stress-strain state of a bridge structure // Vest. Himself. tech. un-that. *Phys.-mat. Science* No. 19 (2003): 80-85.
10 Akhtyamov A.M., Muftakhov A.V. Tikhonov's correctness of the problem of identification of fixings of mechanical systems // *Siberian Journal of Industrial Mathematics* / October-December Vol. XV, No. 4 (52) (2012): 24-37.

11 Ilgamov M.A. Oscillations of elastic shells containing liquid and gas. – Moscow: Nauka (1969).

12 Thompson J.M.T. Instabilities and disasters in science and technology: Per. from English – M .: Mir (1985): 254.

13 Vibration in Technology: A Handbook. T. 1. Ed. V.V. Bolotina. – M.: *Mechanical Engineering* (1978): 352.

14 L. Collatz. Eigenvalue problems (with technical applications). – M.: Nauka (1968): 503.

15 Akhtyamov A.M. On the coefficients of expansions in eigenfunctions of boundary value problems with a parameter in the boundary conditions // *Matematicheskie zametki* Vol. 75, No. 4 (2004): 493-506.

D.B. Zhakebayev, B.A. Satenova*, D.S. Agadayeva

National Engineering Academy of the Republic of Kazakhstan, Almaty, Kazakhstan
*e-mail: satenova.bekzat89@gmail.com

LATTICE- BOLTZMANN METHOD
FOR SIMULATING TWO-COMPONENT FLUID FLOWS

Abstract. In this work, a model of binary fluids with different densities and viscosities based on the solution of the Navier-Stokes equations, the continuity and the Cahn-Hilliard equation is developed. The process of influence of surface tension and interface thickness on the phase fields of fluids is investigated. The numerical results of the study are obtained on the basis of a phase field model using the lattice Boltzmann method (LBM). The LME uses two sets of distribution functions for incompressible flow: one for tracking the pressure and velocity fields and the other for the phase field. The use of the pressure distribution function can significantly reduce the effect of numerical errors in calculating the interfacial force. A several 2D tests are carried out to demonstrate the validation, which included droplet problem and the Raleigh- Taylor instability. It is shown that the proposed method allows tracking the interface with high accuracy and stability.

Key words: phase field, binary fluid, surface tension, chemical potential, lattice Boltzmann method.

Introduction

Numerical modeling of multiphase fluid flows plays an important role in solving many applied scientific and engineering problems, including, for example, oil and gas production, chemical processing of raw materials, and steam-water mixture flows in boilers and condensers. In recent years, more and more attention has been paid to such problems due to their importance for the development of digital microfluid and the development of the laboratory of liquid crystals, gels, suspensions, and also some other technologies. Thus, the study of multiphase fluid flows is an urgent task today.

Interface tracking is widely used in two-phase flow models, which can be divided into two categories: sharp interface methods such as volume-of-fluid methods, level-sets and front-tracking methods, diffuse interface methods. The diffuse interface approach [1] has some advantages over the others in terms of maintaining mass conservation and in the ability of resolving interface curvature with higher accuracy. The main idea of diffuse interface models is to replace sharp interfaces with transition regions of a thin but nonzero layer of thickness, where density, viscosity and other physical quantities smoothly change from the values of one fluid to the values of another.

Among diffuse interface methods, the phase field method [4-5] has become a widely used method in traditional computational fluid dynamics (CFD) and lattice Boltzmann equations (LBM) methods for numerical investigation of complex interphase dynamics. In the phase field method, the thermodynamic behavior of liquids is expressed using the free energy functional of the continuous order parameter [2], which acts as a phase field to distinguish between two-phase fluids. The phase separation equation is formulated for the order parameter that defines the Cahn-Hilliard equation [13].

The concept of a diffuse interface was first proposed by [7], but it has gained popularity only in recent years as a tool for the numerical simulation of two-phase flows. There are many works on the study of multiphase models using various numerical methods [9-12]. The motion of a two-dimensional droplet using a stepwise wettability gradient (WG) was studied in [3]. Also, the diffuse boundary method for simulating the phase separation of complex viscoelastic fluids was investigated in [6] and a model of a binary fluid with free energy for the three-dimensional Bretherton problem (flow between parallel plates) performed in [8]. All of these works have a different modeling approach for boundary tracking and phase separation of liquids with different densities and viscosities. The main difference between these works is the choice of methods for numerical implementation.

In this paper, we introduce multiphase flow model for incompressible binary fluids, when interface between the different phases is tracked by LBE. To simulate phase interface, we derive free-energy based phase field method. To distinguish transition between different phases we set order of parameter ϕ. Also we obtain the numerical implementation of influence surface tension force (σ) and interface thickness (W) on the phase field.

Statement of the problem

To check the numerical algorithm, the results obtained within the framework of solving this problem were compared with the results obtained experimentally, which showed good agreement.

A mixture of two immiscible incompressible fluid in a rectangular region Ω with densities ρ_A, ρ_B and dynamic viscosity η_A, η_B is considered (Figure 1). For the computational domain, a two-dimensional

rectangle with the corresponding dimensional parameters was taken: $x \in [0,1]$, $y \in [0,1]$. In the center of the area $x \in [0.2, 0.8]$, $y \in [0.4, 0.6]$ is situated a liquid drop with density ρ_A and viscosity η_A.

To distinguish the two different fluids, the order of parameter (phase field function) is introduced

$$\phi = \begin{cases} \phi_A, & fluid \ A \\ \phi_B, & fluid \ B \end{cases}$$

For a system of binary fluids, the Landau free energy function F can be defined on the basis of ϕ as:

$$F(\phi, \nabla\phi) = \int_V [\Psi(\phi) + \frac{k}{2}|\nabla\phi|^2]dV$$

where $\Psi(\phi)$ –the bulk free energy density, for an isothermal system the following form can be used $\Psi(\phi) = \beta(\phi - \phi_A)^2(\phi - \phi_B)^2$, k – is the coefficient of surface tension, β – is the coefficient depending on the interface thickness and the surface tension force.
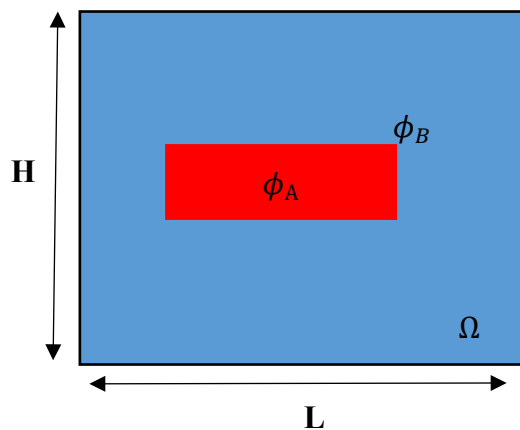

Figure 1 – Computational domain of bubble immersed in liquid

The basic equations for the phase field consist of the continuity equation, the momentum equation for the mixture and the covective Cahn-Hillart equation:

$$\frac{\partial u}{\partial x} + \frac{\partial v}{\partial y} = 0$$

$$\rho(\frac{\partial u}{\partial t} + u\frac{\partial u}{\partial x} + v\frac{\partial u}{\partial y}) = -\frac{\partial P}{\partial x} - \phi\frac{\partial \mu}{\partial x} + \eta\left(\frac{\partial^2 u}{\partial x^2} + \frac{\partial^2 u}{\partial y^2}\right)$$

$$\rho(\frac{\partial v}{\partial t} + u\frac{\partial v}{\partial x} + v\frac{\partial v}{\partial y}) = -\frac{\partial P}{\partial y} - \phi\frac{\partial \mu}{\partial y} + \rho g + \eta\left(\frac{\partial^2 v}{\partial x^2} + \frac{\partial^2 v}{\partial y^2}\right)$$

$$\frac{\partial \phi}{\partial t} + \frac{\partial (\phi u)}{\partial x} + \frac{\partial (\phi v)}{\partial y} = M\left(\frac{\partial^2 \mu}{\partial x^2} + \frac{\partial^2 \mu}{\partial y^2}\right)$$

where u,v – are the velocity components, p – is the pressure, $\rho = \frac{\phi - \phi_B}{\phi_A - \phi_B}\rho_A + \frac{\phi_A - \phi}{\phi_A - \phi_B}\rho_B$ – is the density, here ρ_A, ρ_B – are the density of fluids, $\eta = \frac{\eta_A \eta_B (\phi_A - \phi_B)}{(\phi - \phi_B)\eta_B + (\phi_A - \phi)\eta_A}$, here $\eta_A = \rho_A \vartheta_A, \eta_B = \rho_B \vartheta_B$ – are the dynamic viscosity, ϑ_A, ϑ_B – are the kinematic viscosity, ϕ – is the phase field function, g – is the acceleration of gravity, M – is the mobility coefficient, μ- is the chemical potential, $F_x = -\phi \frac{\partial \mu}{\partial x}$, $F_y = -\phi \frac{\partial \mu}{\partial y}$ are the surface tension force, $F_b = \rho g$ is the acceleration force.

The variation of the free- energy function F with respect to the function ϕ is solving chemical potential μ as :

$$\mu = \frac{\delta F}{\delta \phi} = \frac{d\Psi}{d\phi} - k\nabla^2 \phi =$$
$$= 4\beta(\phi - \phi_A)(\phi - \phi_B)(\phi - \frac{\phi_A + \phi_B}{2}) - k\nabla^2 \phi,$$

where $W = \frac{1}{|\phi_A - \phi_B|}\sqrt{\frac{8k}{\beta}}$- is the interface thickness, $\sigma = \frac{|\phi_A - \phi_B|^3}{6}\sqrt{2k\beta}$ – is the surface tension force.

The system of equations has the following initial and boundary conditions:

$$u = 0, v = 0, \phi =$$
$$= \begin{cases} \phi_A, & x,y \notin \Omega \\ \phi_B, & x,y \in \Omega \end{cases} at\ t = 0, 0 \leq x \leq L, 0 \leq y \leq H$$

$$u = 0, v = 0, \frac{\partial \phi}{\partial x} =$$
$$= 0\ at\ x = 0\ и\ x = L, 0 \leq y \leq H$$

$$u = 0, v = 0, \frac{\partial \phi}{\partial y} = 0\ at\ y = 0$$
$$и\ y = H, 0 \leq x \leq L$$

Numerical method

We use the lattice Boltzmann equation (LBE) to describe the motion of binary fluids. For this case, the collision term LBM in a two-dimensional square lattice with nine velocities (D2Q9) was used. The lattice Boltzmann equation in the Batnagar-Gross-Krook (BGK) [15] approximation is as follows:

$$f_i(x + e_i\Delta t, t + \Delta t) - f_i(x, t) =$$
$$= -\left(\frac{f_i(x,t) - f_i^{eq}(x,t)}{\tau_f}\right) + (1 - \frac{\Delta t}{2\tau_f})F_i(x,t)\Delta t$$

$$g_i(x + e_i\Delta t, t + \Delta t) - g_i(x, t) =$$
$$= -\left(\frac{g_i(x,t) - g_i^{eq}(x,t)}{\tau_\phi}\right) +$$
$$+\Gamma[g_i^{eq}(x + e_i\Delta t, t) - g_i^{eq}(x, t)]$$

where f_i, g_i – are the velocity and phase field distribution function respectively, e_i- is a discrete lattice velocity, τ_f, τ_ϕ- are the relaxation time for the velocity and phase field respectively, F_i- is a force term, $\Gamma = 2\tau_\phi - 1$ constant controlling the mobility, Δt - is a time step, f_i^{eq}, g_i^{eq} – are the equilibrium distribution function for the velocity and phase field respectively.

The equilibrium distribution functions are introduced as following:

$$f_i^{eq} =$$
$$= \begin{cases} -(1 - w_0)\frac{p}{c_s^2} - w_0 \frac{u \cdot u}{2c_s^2}, i = 0 \\ w_i p + c_s^2 \rho w_i \left[\frac{e_i \cdot u}{c_s^2} + \frac{(e_i \cdot u)^2}{c_s^4} - \frac{u^2}{2c_s^2}\right], i \neq 0 \end{cases}$$

$$g_i^{eq} = \begin{cases} \phi - \frac{(1 - w_0)\Gamma\mu}{(1 - \Gamma)c_s^2}, i = 0 \\ w_i \frac{\Gamma\mu + (e_i u)\phi}{(1 - \Gamma)c_s^2}, i \neq 0 \end{cases}$$

where $c_s^2 = \frac{1}{3}$ - is a lattice sound speed, $p_b = c_s^2\rho + \beta(-\frac{1}{2}\phi^2 + \frac{3}{4}\phi^4)$ - is a pressure of a mixture.

For the D2Q9 model, discrete velocities are calculated as:

$$e_{ix} = (0,1,1,0,-1,-1,-1,0,1)c$$

$$e_{iy} = (0,0,1,1,1,0,-1,-1,-1)c$$

The values of the weighting parameters are defined as:

$$w_i = \begin{cases} \dfrac{4}{9} & i = 0 \\ \dfrac{1}{9} & i = 1,2,3,4 \\ \dfrac{1}{36} & i = 5,6,7,8 \end{cases}$$

In this paper, the scheme proposed by Guo et al. [14] is used to approximate the external force in the LBM:

$$F_i(x,t) = \left(1 - \frac{1}{2\tau}\right) w_i \left(3\frac{c_i - u}{c_s^2} + 9\frac{c_i - u}{c_s^4} c_i\right) F$$

where, $F = (F_x + F_y + F_b)$

The evolution equation is divided into two steps, collision and propagation:

1. $f_i^*(x,t) = f_i(x,t) - \frac{\Delta t}{\tau_f}\Big(f_i(x,t) - f_i^{eq}(x,t)\Big) + (1 - \frac{\Delta t}{2\tau_f})F_i(x,t)\Delta t$

$f_i(x + c_i\Delta t, t + \Delta t) = f_i^*(x,t)$

2. $g_i^*(x,t) = g_i(x,t) - \frac{t}{\tau_\phi}(g_i(x,t) - g_i^{eq}(x,t))$

3. $g_i(x + c_i\Delta t, t + \Delta t) = g_i^*(x,t)$

After the second step, we update the macroscopic parameters (density, phase field, velocity) using the following formulas:

$$\rho = \sum_i f_i, \rho u_\alpha = \sum_i f_i c_\alpha + \frac{F\Delta t}{2}, \phi = \sum_i g_i$$

The following boundary conditions were used to close the system of equations.

Zero velocity condition for all walls:

$$f_i(x_w, t + \Delta t) = f_{-i}(x_w, t + \Delta t),$$
$$e_i \cdot n > 0,$$

Neumann condition for phase filed on all walls:

$$g_i(x_w, t + \Delta t) = g_{-i}(x_w, t + \Delta t),$$
$$e_i \cdot n > 0,$$

Numerical results and discussions

First we performance, the numerical calculations of problem where, a stationary droplet immersed in another fluid. This task is used to assess the capability of the proposed model in handling the surface force. Initially, a round drop with a radius of 20 (in lattice units) is placed in the center of a square computational domain with a size of 100x100.

Table 1 – Modeling parameters

Parameters	Physical parameters	LBM parameters
Characteristic length	$L_{char} = 0.01$	
Number of points by x, y	$N_x \times N_y = 128 \times 256$	
Kinematic viscosity	$\vartheta = \dfrac{\eta}{\rho}$	$\vartheta = c_s^2(\tau - \dfrac{1}{2})\dfrac{\Delta x^2}{\Delta t}$
Characteristic time	$T_{char} = \sqrt{\dfrac{L_{char}}{g_{char} * At}}$	$\tau = c_s^2(\tau - \dfrac{1}{2})\dfrac{\Delta x^2}{\vartheta}$
Maximum velocity	$U_{char} = \sqrt{L_{char} g_{char}} = 0{,}31305$	$U_{lbm} = \dfrac{U_{char}}{c_u}, c_u = \dfrac{\Delta x}{\Delta t}$
Mixture density	$\rho_{A.char} = 800, \rho_{B.char} = 600$	$\rho_A = \dfrac{\rho_{A.char}}{\rho_{A.char}}, \rho_B = \dfrac{\rho_{B.char}}{\rho_{A.char}}$
Dynamic viscosities of fluids A and B	$\eta_{A.char} = 0.02, \eta_{B.char} = 0.01$	$\eta_A = \dfrac{\eta_{A.char}}{\eta_{char}} \; \eta_B = \dfrac{\eta_{B.char}}{\eta_{char}}$

Model parameters are set as: $\tau_f = \tau_\phi = 1, \phi_A = 1, \phi_B = -1, \rho_A = 1, \rho_B = 0.7$. The basic dimensionless parameters for the droplet problem are shown in table 1.

The time step was taken $\Delta t = 0.0001$ seconds. In numerical simulation, when interface width W and the surface tension σ are given, the coefficients k and β can be determined as follows:

$$k = \frac{3\sigma W}{8}, \beta = \frac{3\sigma}{4W}$$

The numerical solution showed that with decrease the coefficient σ of surface tension, leads to decrease a chemical tension of the phases, as shown in Figure 2.
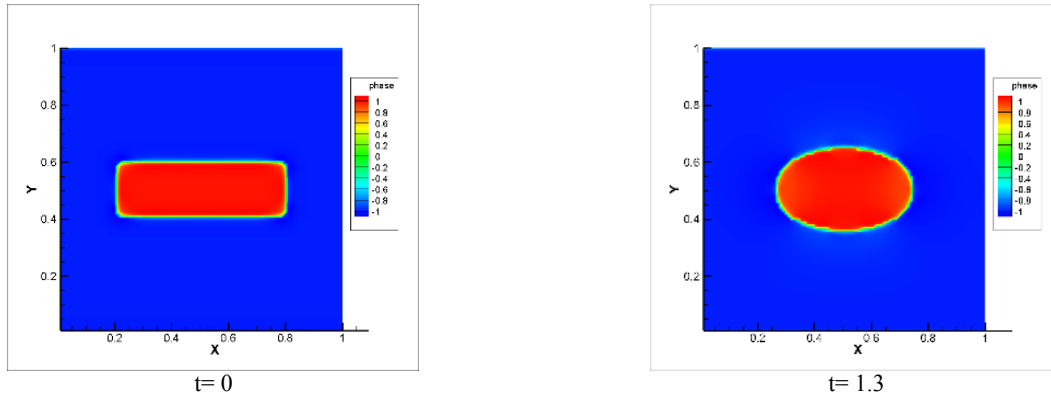

Figure 2 – The dynamics of the change in the shape of a drop in a fluid at different time
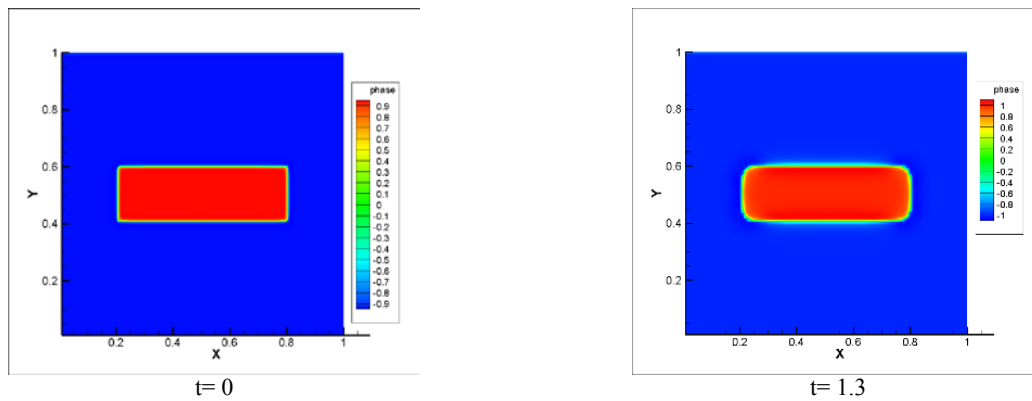for $\sigma = 0,01, W = 1$. The time normalized by characteristic time T_{char}

Figure 3 – The dynamics of the change in the shape of a drop in a fluid
at different time for $\sigma = 0,001, W = 1$. The time normalized by characteristic time T_{char}

Figure 3 shows when surface tension σ is decrease , the force of surface attraction decreases and the shape of the drop does not change. In addition, with an increase interface thickness coefficient W, the surface tension β decreases, which contributes to a more rapid formation of a ball-like shape, as shown in Figure 4.

To further demonstrate the ability of this model to solve more complex flows, we simulated the Rayleigh-Taylor instability, which occurs when there is a small disturbance at the interface between a heavy (fluid A) and a light fluid (fluid B).

The basic dimensionless parameters for the Rayleigh-Taylor instability problem are shown in table 1. The initial interface between the two fluids is shown in Figure 5 (t=0). Reflection boundary conditions are applied to the lower and upper boundaries, and periodic boundary conditions are applied to the side boundaries. In our simulations, the physical parameters are fixed as:

$$U_{char} = 0.04, W = 4, \sigma = 0.1,$$

$$Re = \frac{\rho_{char} U_{char} L_{char}}{\eta_{char}}, At = \frac{\rho_{A.char} - \rho_{B.char}}{\rho_{A.char} + \rho_{B.char}} = 0.1$$
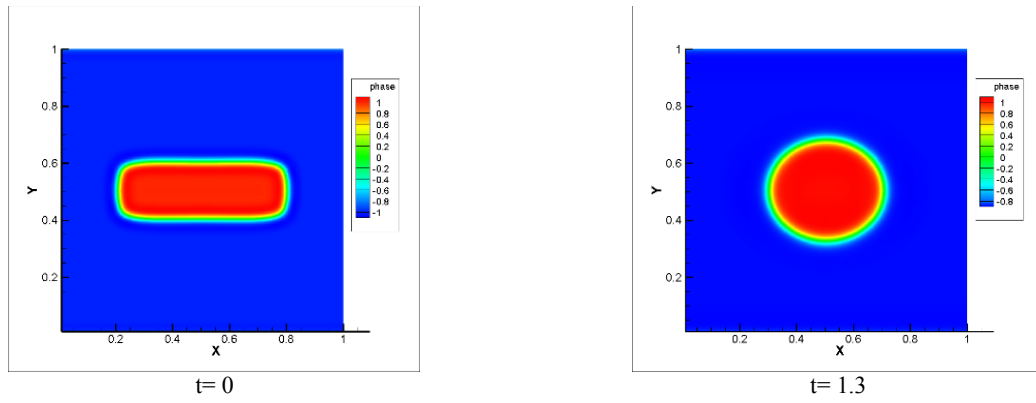
Figure 4 – The dynamics of the change in the shape
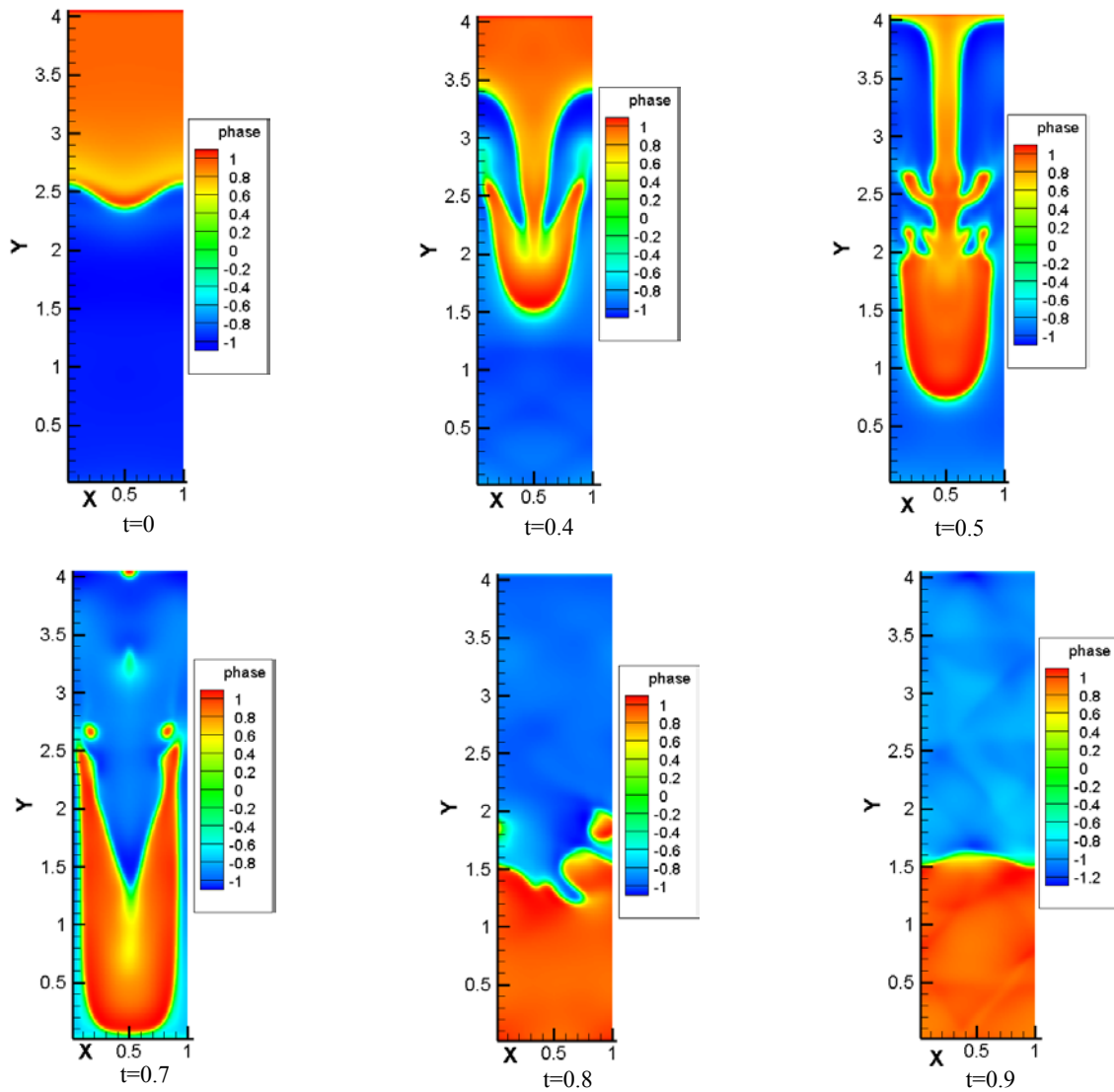of a drop in a fluid at different time for $\sigma = 0,01, W = 4$

Figure 5 – Dynamics of concentration separation in the fluid phase at different times

In the early stages, the growth of the fluid interface remains symmetrical up and down. Later, the heavy liquid settles down, and the light fluid rises, forming bubbles. Starting from t = 0.4 (Fig. 5), the heavy fluid begins to curl up into two oncoming vortices. These discontinuities disappear over time, as at t = 0.7 , the Rayleigh-Taylor instability appears. At t = 0.9 , it can be seen that the heavy fluid has completely settled, and the light fluid has gone up. Thus, the problem of the Rayleigh-Taylor instability describes well the process of settling of a heavy fluid.

The problem was also solved for the case when $At = 0.1428, \tau_f = 0.8, \sigma = 0,01, W = 2$. Below in Figures 6- 8 the simulation result is shown, which illustrates the dynamics of concentration separation of a mixture of heavy and light liquids at different times: Figure 6 - for times t = 0; 0.2; 0; 32; 0.36 (from left to right, respectively); Figure 7 - t = 0.4; 0.5; 0.56; 0.6 (left to right, respectively); Figure 8 - t = 0.64; 0.72; 0.74; 0.8 (left to right, respectively). It can be seen from the figures that for the case when a more viscous liquid is considered (the separation boundary of the mixture components is thinner), a slower process of establishing equilibrium is observed - over time, first the formation of vortices occurs, then a rupture of the interface of the liquid boundaries is observed, the formation of separate structures of a fluid of higher density occurs inside a fluid of lower density, the formation of bubbles, the boundary of which breaks over time, equilibrium is established due to the chemical velocity of attraction of the phases.
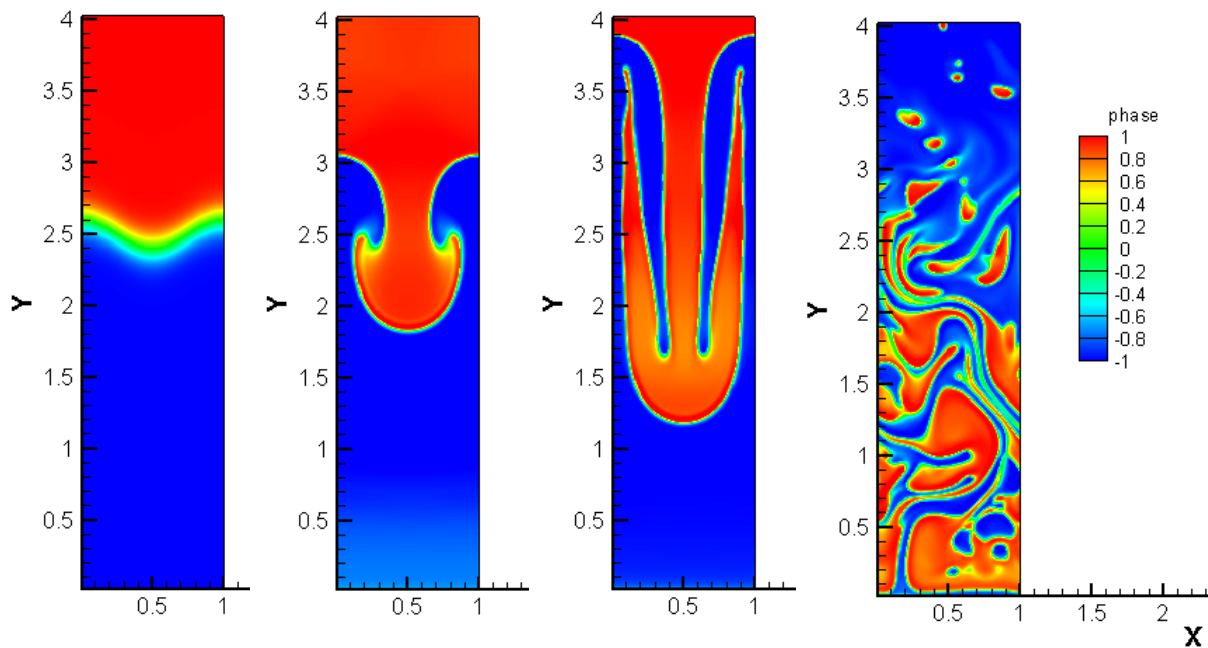

Figure 6 – Dynamics of concentration separation
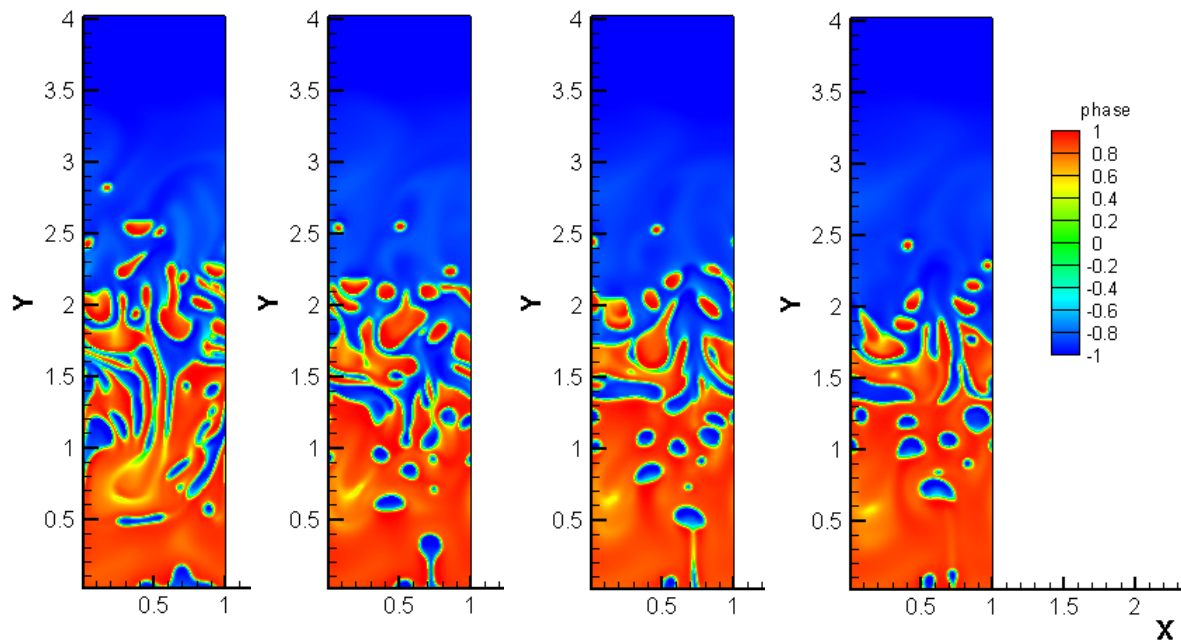in the fluid phase at different times

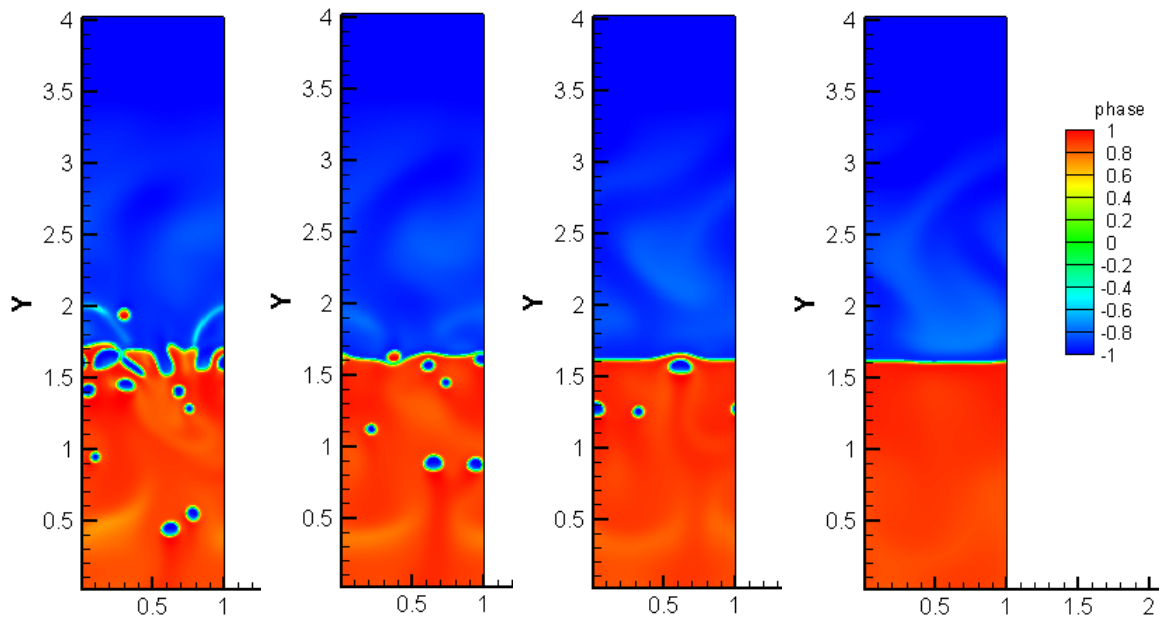**Figure 7** – Dynamics of concentration separation in the fluid phase at different times

Figure 8 – Dynamics of concentration separation in the fluid phase at different times

Thus, a mathematical model has been developed for the separation of components of binary fluids with different density and viscosity. A 2D numerical algorithm based on the D2Q9 model of the lattice Boltzmann method to simulate a multiphase flow of an incompressible fluid in a bounded rectangular cavity is developed. For incompressible flow, two sets of distribution functions are used: one for tracking the pressure and velocity fields, and the other for the phase field. The use of the pressure distribution function makes it possible to significantly reduce the effect of numerical errors in calculating the interfacial force. Numerical modeling was carried out for the two-dimensional Rayleigh - Taylor instability and for the fluid droplet problem. The main conclusion of this problem can be considered the following: if the thickness interface between two immiscible fluids is large, then spherical drops appear faster than in the case when the boundary is thin. In addition, by implementation of the developed mathematical model, the process of mass transfer of two fluids of different density and viscosity in a given area is clearly shown.

Acknowledgement

References

1 P. Yue, J.J. Feng, Ch. Liu, J. Shen. A diffuse-interface method for simulating two-phase flows of complex fluids. *J. Fluid Mech.* № 515 (2004): 293–317.

2 J. W. Cahn, J. E. Hilliard. Free Energy of a Nonuniform System. I. Interfacial Free Energy. *Journal of chemical physics* Vol. 28, №2(1958): 258-267.

3 J.J. Huang, H. Huang, X. Wang. Numerical study of drop motion on a surface with stepwise wettability gradient t and contact angle hysteresis. *Physics of Fluids* № 26 (2014), 062101.

4 J. Shen and X. Yang. Energy stable schemes for Cahn-Hilliard phase-field model of two phase incompressible flows equations. Chinese Annals of Mathematics, Series B, 31B (5) (2010): 743–758.

5 J. Shen and X. Yang. A phase-field model and its numerical approximation for two-phase incompressible flows with different densities and viscosities. *SIAM J. Sci. Comput.* №32 (2010): 1159–1179.

6 Y. Q. Zu and S. He. Phase-field-based lattice Boltzmann model for incompressible binary fluid systems with density and viscosity contrasts. Physical Review E. 87 (2013): 043301.

7 J.D. van der Waals, Verhandel. Konink. Akad. Weten. AmsterdamSect vol. 1 No. 8 (Dutch) (1893), Translation of J.D. van der Waals (The thermodynamic theory of capillarity under the hypothesis of a continuous density variation) *J. Stat. Phys.* (1979).

8 A. Kuzmina, M. Januszewski, D. Eskinc, F. Mostowfic, J.J. Derksena. Three-dimensional binary-liquid lattice Boltzmann simulation of microchannels with rectangular cross sections. *Chemical Engineering Journal* №178 (2011): 306-316.

9 T. Ménard, S. Tanguy, A. Berlemont Coupling level set/VOF/ghost fluid methods: Validation and application to 3D simulation of the primary break-up of a liquid jet. *Int. J. Multiphase Flow* №33 (2007): 510–524.

10 Ch. Zhang, K. Yang, Zh. Guo. A discrete unified gas-kinetic scheme for immiscible two-phase flows. Int. J. Heat & Mass. Transfer. № 126 (2018): 1326–1336.

11 H. Kusumaatmaja, E.J. Hermingway, S. M. Fielding. Moving contact line dynamics: from diffuse to sharp interfaces. *J. Fluid Mech.* 778 (2016): 209-227.

12 T. Inamuro, T. Ogata, S. Tajima, N. Konishi. A lattice Boltzmann method for incompressible two-phase flows with large density differences. J. Comput. Phys. 198 (2) (2004): 628–644.

13 D. Jacqmin. Calculation of two- phase Navier-Stokes flows using phase- filed modeling. Journal of Computational Physics 155(1999): 96-127.

14 Z. Guo, C. Zheng, B. Shi. Discrete lattice effects on the forcing term in the lattice Boltzmann method. Phys. Rev. E. № 65 (2002): 1–6.

15 P.L. Bhatnagar, E.P. Gross, M. Krook. A model for collision processes in gases. I. Small amplitude processes in charged and neutral one-component systems. Phys. Rev. 94 (3) (1954): 511-525

Zh.M. Moldabekov[1*], A.M. Zhukeshov[1], V.Ya. Nikulin[2], I.V. Volobuev[2]

[1] National Nanotechnology Laboratory of Open Type, Almaty, Kazakhstan
[2] P.N. Lebedev Physical Institute of Russian Academy of Sciences, Moscow, Russia
*e-mail: Zhan.moldabek@gmail.com

STUDY NEUTRON EMISSION IN PLASMA FOCUS DEVICE BY SILVER ACTIVATION METHOD

Abstract. Dense Plasma Focus machine may be suitable for fusion first wall studies and its related material researches. As is well-known plasma focus devices are sources of high energy ions, electrons, x-rays and neutrons and intense bursts of fast plasma streams. In this paper, experimental measurements of neutron emission and hard x-ray emission from the plasma focus device are presented. The measurement of neutron and hard x-ray emission is studied using silver activation counter detector with two different dimensions Pb shielding and two scintillator photomultiplier detector systems. The research paper reported that the experimentally detected neutron emission in the radial direction where focus occurs also evaluated neutron fluency at different distances. The results show that neutron emission with different intensities and pulse width. Silver detector registered neutrons in the range 10^6-10^7 n/shot in the radial direction. The maximum neutron yield is 1.7×10^7 neutrons per shot.
Key words: neutron yield, plasma focus, X-ray, shielding, silver foil, photo multiplier tube.

Introduction

The dense plasma focus or simply the plasma focus is a device that can induce nuclear reactions using electromagnetic force generated between electrodes. The phenomenon of "plasma focus" was discovered independently in the middle of the twentieth century by N.V. Filippov (USSR) [1] and J. Mather (J. Mather, USA) [2] in the studies conducted under the program of controlled thermonuclear fusion. Plasma focus attracted the attention of researchers when the working chamber was filled isotope of hydrogen–deuterium, the intensity of accelerated (fast) ionic and electronic particles inside the chamber generates a powerful short pulse of fast neutrons and X-rays.

It is well known that neutron is an uncharged particle and does not interact directly with the electrons of matter and hence it is difficult to detect it directly. Therefore to detect neutrons it is necessary to use indirect methods such as recoil technique or nuclear reactions. The foil activation technique is also used for detecting neutron [3]. In this technique the neutron is allowed to be absorbed by the nucleus to from a compound nucleus. The measure of particles emitted from the compound nucleus such as beta or gamma radiation. The method of foil activation by neutrons is one of the best methods to measure neutron flux [5,6].

The Neutron activation method and silver activation detectors are widely used in measurements of neutron yield and neutron flux parameters in plasma focus. In practice, it is the only method that allows measurements of neutron field parameters in a wide energy range (from thermal to 20 MeV) [9]. The activation method is widely used as a diagnostic technique for neutron yield registered in pulsed thermonuclear sources. In early plasma focus (PF) research papers [4-7], activation of Silver foil has been used and the so-called silver activated Geiger counter is the most known and accuracy detector. In PF devices, depending on the filling gas, neutrons from D−D reactions are produced with typical energies of 2.45MeV. Silver activation detectors are usually converted fast neutrons to thermal neutrons. Nonetheless, activation by fast neutrons could be used as the Indium or Beryllium counters when neutron intensity is high enough, typically higher than 10^8 n per source pulse [8].

The use of plasma focus in thermonuclear reactors was considered in [4,6]. The present-day level of understanding of these processes opens new perspectives for creation of a fusion reactor based on the new data. Therefore, it is necessary to study the

possibility of creating an alternative type of thermonuclear reactor at the plasma focus installations and to conduct experiments on existing installations. Experimentally measurements of the neutron yield and use it modern technology an essential and important part of our research. In this paper, the problem is posed experimentally to measure neutron yield by activation method.

Method of investigation

The experiment was carried out plasma focus PF-4 which cylindrical coaxial electrodes: anode and cathode (length of anode and cathode 33 mm and 38 mm respectively). The insulator used is a 31 mm long ceramic. The energy storage system of the PF-4 includes a capacitor bank of capacitance 20 µF with a working voltage of 10–20 kV and 2.6–280 nH [7, 9]. High voltage is switched using a controllable discharger (air-filled). The results in this work were obtained by charging the capacitor bank at 14-18 kV. To study the characteristics of neutron emission we used activation detectors which were previously calibrated with an Am–Be source and a photomultiplier tube (PMT) with a plastic scintillator.

A typical neutron activation detector consists of a block of a hydrogen-containing fast neutron moderator, inside which a silver foil is placed. The silver foil is wrapped around the Geiger counter, which registers β- activity induced by slow neutrons. This type of sensor has a relatively large "dead time" (~100 µs). Let the detector be irradiated with fast (2.5 MeV) neutrons from a constant source of intensity I (neutron/s), located at the point from which the detector is visible at a solid angle Ω. After the irradiation process, the activity of the wrapped foil $A(t_2)$ will be equal to [7,10]:

$$A(t_2) = n\overline{V}\Sigma(\overline{V})d(1 - e^{-t_1/T}) \qquad (1)$$

Then the expression (1) can be rewritten:

$$N = I\left(\frac{\Omega}{4\pi}\right)\varepsilon T\left(1 - e^{-t_1/T}\right)e^{-t_2/T}\left(1 - e^{-\Delta t/T}\right) \qquad (2)$$

where ψ is the coefficient of proportionality characterizing the efficiency of registration of β particles by the Geiger counter, T is the radioactivity relaxation time, Σ is the activation cross-section, d is the activated plate thickness($\Sigma d \ll 1$), ε is the detector efficiency, t_1 is the radiation time of the foil, t_2 is the time interval between the end of irradiation and start of counting, Δt is the measurement time, I is the intensity of the neutron source, Ω is a solid angle at which the detector is visible from the point where the pulsed neutron source is formed, N is the number of pulses, Y is the neutron yield.

Results and Discussion

To measure the neutron flux in the radial direction silver activation detectors were located at distances at 16 cm and 26 cm. The centers of the detectors were placed at the same height and were shielded by the lead sheet of thickness 1.2 mm and 2.5 mm to avoid activation by hard x-rays. We evaluated the angular differential neutron yields at the distances of 16 cm and 26 cm from the electrode where compression of plasma occurs. The comparison of the neutron yields is shown in Fig. 1.
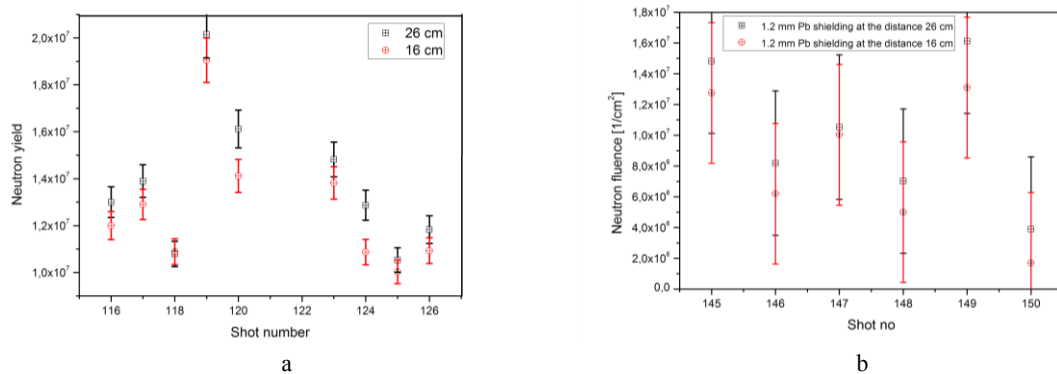

a

b

Figure 1 – Neutron yield and neutron fluence in the radial direction
at the distance of 16 cm and 26 cm: *a* – without shielding, *b* – with shielding

The maximum neutron yield Y in the present case roughly matches the scaling law $Y \sim I^4$ (I in kA) proposed by early researchers [7]. To evaluate the dependence of the neutron emission on the filling gas pressure, the neutron signals (PMT) and neutron counts (by SAC) were recorded by varying the filling gas pressure from 2 to 10 Torr. The neutron emission reduces dramatically with variation in pressure in the experimental device. This might be explained by the fact that with an increase in pressure, the role of the beam mechanism in the neutron production decreases.

Two scintillator-photomultiplier systems have been used for hard X-ray and neutron measurement. The temporal evolution in neutron and X-ray pulse with respect to the dI/dt dip was obtained using PMT (Fig. 2).
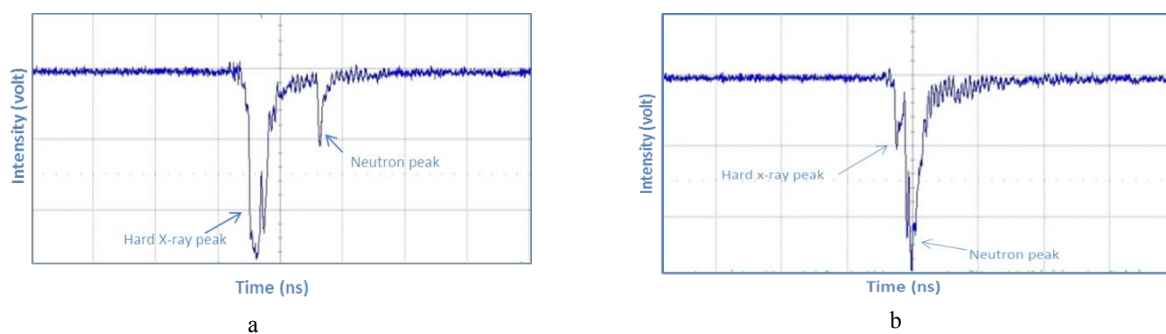
Figure 2 – Typical neutron signal obtained by PMT:
a – weak neutron and strong hard X-ray signals without lead sheet;
b – strong neutron and weak hard X-ray signal capture with lead sheet

The PMT was placed at distances 1.5 and 1.9 meters away from the tip of the central electrode in its radial direction. It is noted that both PMT signals give two distinct pulses as shown in Fig.2. The first pulse in both PMT signals appears at the same time, while the second pulses appear with a time difference of around 100 ns. From this observation, one can conclude that the first pulse is due to hard X-ray emission, as it appears at the same time in both signals. The generation of this hard X-ray is due to the bombardment of the anode surface by an energetic electron beam [11-12]. The second pulse is thought to be a result of emission of an energetic particle as it took time to reach the PMT. Since the particles penetrated the plasma focus chamber wall, it must be due to neutron emission. To make the results more precise, both detectors had shielding (Pb filters) of thickness 1.2 mm and 2.5 mm in front of the PMT and their signals were monitored. The shielding considerably reduced the first pulse leaving the second pulse almost the same. The shielding of thickness 1.2 mm can significantly attenuate hard X-rays, but the attenuation is insignificant for the neutron (Fig.2c). In some of the PMT signals, it is observed that the neutron pulse is very intense in amplitude with a small pulse of hard X-ray, while in some cases, the opposite result is obtained, i.e. a small neutron pulse with an intense hard X-ray pulse (Fig.2a and 2b).

Conclusion

The neutron emission has been studied using a PF-4 device operating in the deuterium medium by using PMT and a silver foil detector. The results show two pulses of neutron emission with different intensities and pulse width. Depending on the relative proportion of ion and electron currents or time of their existence the PF device will emit more intense hard X-ray or more intense neutron pulse. The neutron emission is found to be strongly dependent on the operating pressure and it was the highest at around 7,5-8 Torr. The corresponding pinching time is observed near the maximum of discharge current and thus transfers the maximum energy into the plasma. Therefore, the neutron emission is the highest at this pressure. The maximum neutron yield of $1,7 \times 10^7$ neutrons per shot has been achieved for the silver detector. These experiments detected neutrons in the range 10^6-10^7 n/shot in the radial direction. The measurement of neutron fluency ($2 \cdot 10^6$-$1.7 \cdot 10^7$ n/cm^2) at different distances from the pinch in the radial direction shows that the DD neutrons are mainly emitted in the axial direction. In

our case, the registered particles were 6.4×10^6 – $1,4 \times 10^7$ neutrons per shot and velocity 2,625-8,75 cm/µs. The obtained results can use experimental study basic problems for all fusion facilities.

References

1 J. Mather. "Investigation of the high-energy acceleration mode in the coaxial gun", *Physics of Fluids 7,* (1964).

2 N. Filippov, T. Filippova, V. Vinogradov. "Dense high-temperature plasma in a non-cylindrical z – pinch compression", *Plasma,* (1962).

3 N.V. Filippov, T.I. Filippova, I.V. Khutoretskaia, V.V. Milton, V.P. Vinogradov. "Megajoule Scale Plasma Focus as Efficient X-ray Source", *Physics Letters A, 211* (1996).

4 J.M. Koh, R.S. Rawat, A. Patran, T. Zhang, D. Wong, S.V. Springham, T.L. Tan, S. Lee and P. Lee "Optimization of the high pressure operation regime for enhanced neutron yield in a plasma focus device" *Plasma Sources Science and Technology,* (2003)

5 R.K. Cherdizov et al. "Experimental research of neutron yield and spectrum from deuterium gas-puff z-pinch on the GIT-12 generator at current above 2 MA", *Phys.: Conf. Ser. 830* (2017).

6 N. Talukdar, N.K. Neog, and T.K. Borthakura. "Study on neutron emission from 2.2 kJ plasma focus device", *Physics of Plasmas*, (2014).

7 O.N. Krokhin, V.Ya. Nikulin, M. Scholz, I.V. Volobuev. "The Measurements of Neutron Emission on Plasma Focus Installations with Energy Ranging from 4 to 1000 kJ", *Proc. of 20th Symp. on Plasma Physics and Technology,* (2002).

8 Ariel Tarifeno-saldiva, Roberto E. Mayer, Cristian Pavez and Leopoldo Soto. "Methodology for the use of proportional counters in pulsed fast neutron yield measurements" (2011).

9 A.M. Zhukeshov, B.M. Ibraev, Sh.G. Giniyatova, B.M. Useinov, V.Ya. Nikulin, A.T. Gabdullina, A.U. Amrenova "Parameters calculation and design of vacuum camera for «Plasma Focus» facility", *International Journal of Mathematics and Physics, 1* (2016).

10 O.N. Krokhin, V.Ya. Nikulin, I.V. Volobuev. "Compact activation detectors for measuring of absolute neutron yield generated by powerful pulsed plasma installations", *Czech. J. Phys., 54* (2004).

11 I. Murata, I. Tsuda, R. Nakamura, S. Nakayama, M. Matsumoto H. Miyamaru. "Neutron and gamma-ray source-term characterization of Am-Be sources in osaka university", *Progress in Nuclear Science and Technology, 4* (2014).

12 A. Zhukeshov, A. Amrenova, A. Gabdullina, Z. Moldabekov "Calculation and Analysis of Electrophysical Processes in a High-Power Plasma Accelerator with an Intrinsic Magnetic Field", *Technical physics, 62 N.3*(2019).

Contents